TUMOR IMMUNOLOGY

Targeted deletion of PD-1 in myeloid cells induces antitumor immunity

Laura Strauss[1,2,3], Mohamed A. A. Mahmoud[1,2,3]*, Jessica D. Weaver[1,2,3], Natalia M. Tijaro-Ovalle[1,2,3], Anthos Christofides[1,2,3], Qi Wang[1,2,3], Rinku Pal[1,2,3], Min Yuan[3], John Asara[3], Nikolaos Patsoukis[1,2,3], Vassiliki A. Boussiotis[1,2,3]†

PD-1, a T cell checkpoint receptor and target of cancer immunotherapy, is also expressed on myeloid cells. The role of myeloid-specific versus T cell–specific PD-1 ablation on antitumor immunity has remained unclear because most studies have used either PD-1–blocking antibodies or complete PD-1 KO mice. We generated a conditional allele, which allowed myeloid-specific (PD-1$^{f/fLysMcre}$) or T cell–specific (PD-1$^{f/fCD4cre}$) targeting of *Pdcd1* gene. Compared with T cell–specific PD-1 ablation, myeloid cell–specific PD-1 ablation more effectively decreased tumor growth. We found that granulocyte/macrophage progenitors (GMPs), which accumulate during cancer-driven emergency myelopoiesis and give rise to myeloid-derived suppressor cells (MDSCs), express PD-1. In tumor-bearing PD-1$^{f/fLysMcre}$ but not PD-1$^{f/fCD4cre}$ mice, accumulation of GMP and MDSC was prevented, whereas systemic output of effector myeloid cells was increased. Myeloid cell–specific PD-1 ablation induced an increase of T effector memory cells with improved functionality and mediated antitumor protection despite preserved PD-1 expression in T cells. In PD-1–deficient myeloid progenitors, growth factors driving emergency myelopoiesis induced increased metabolic intermediates of glycolysis, pentose phosphate pathway, and TCA cycle but, most prominently, elevated cholesterol. Because cholesterol is required for differentiation of inflammatory macrophages and DC and promotes antigen-presenting function, our findings indicate that metabolic reprogramming of emergency myelopoiesis and differentiation of effector myeloid cells might be a key mechanism of antitumor immunity mediated by PD-1 blockade.

INTRODUCTION

Programmed cell death protein 1 (PD-1) is a major inhibitor of T cell responses expressed on activated T cells. It is also expressed on natural killer cells, B cells, regulatory T cells, T follicular helper cells, and myeloid cells (*1*). The current model supports that a key mechanism dampening antitumor immune responses is the up-regulation of PD-1 ligands in cancer cells and antigen-presenting cells (APCs) of the tumor microenvironment (TME), which mediate ligation of PD-1 on tumor-infiltrating CD8$^+$ T cells, leading to the development of T incapable of generating antitumor responses (*2*). Therapeutic targeting of the PD-1 pathway with antibodies blocking the PD-1 receptor or its ligands induces expansion of oligoclonal CD8$^+$ tumor-infiltrating lymphocytes that recognize tumor neoantigens (*3*). Thus, in the context of cancer, PD-1 is considered a major inhibitor of T effector cells, whereas on APC and cancer cells, emphasis has been placed on the expression of PD-1 ligands. PD-1 ligand-1 expression in the TME is often a prerequisite for patient enrollment to clinical trials involving blockade of the PD-1 pathway. However, responses do not always correlate with PD-L1 expression, and it remains incompletely understood how the components of the PD-1:PD-L1/2 pathway suppress antitumor immunity.

Recent studies indicated that PD-1 can be induced by Toll-like receptor (TLR) signaling in macrophages (MΦ) and negatively correlates with M1 polarization (*4*). PD-1 expression in macrophages plays a pathologic role by suppressing the innate inflammatory response to sepsis (*5*) and inhibiting *Mycobacterium tuberculosis* phagocytosis in active tuberculosis (*6*). Our knowledge about the function of PD-1 on myeloid cells in the context of cancer is very limited. However, similar to its role in infections, PD-1 expression inversely correlates with M1 polarization and phagocytic potency of tumor-associated MΦ (TAM) against tumor (*7*, *8*). The mechanisms of PD-1 expression in myeloid cells and the role of PD-1–expressing myeloid cells in tumor immunity remain unknown.

The rapid increase in myeloid cell output in response to immunologic stress is known as emergency myelopoiesis. Terminally differentiated myeloid cells are essential innate immune cells and are required for the activation of adaptive immunity. Strong activation signals mediated by pathogen-associated molecular pattern or danger-associated molecular pattern molecules lead to a transient expansion and subsequent differentiation of myeloid progenitors to mature monocytes and granulocytes to protect the host. In contrast, during emergency myelopoiesis mediated by continuous low-level stimulation mediated by cancer-derived factors and cytokines, bone marrow common myeloid progenitors (CMPs) but, predominantly, granulocyte/macrophage progenitors (GMPs) undergo modest expansion with hindered differentiation, and a fraction of myeloid cells with immunosuppressive and tumor-promoting properties, named myeloid-derived suppressor cells (MDSCs), accumulates. MDSCs suppress CD8$^+$ T cell responses by various mechanisms (*9*). In the mouse, MDSCs consist of two major subsets, CD11b$^+$Ly6C^{hi}Ly6G$^-$ (thereafter named CD11b$^+$Ly6C$^+$) monocytic (M-MDSC) and CD11b$^+$Ly6C^{lo}Ly6G$^+$ (hereafter named CD11b$^+$Ly6G$^+$) polymorphonuclear (PMN-MDSC) (*10*). These cells have similar morphology and phenotype to normal monocytes and neutrophils but distinct genomic and biochemical profiles (*9*). In humans, in addition to M-MDSC and PMN-MDSC, a small subset of early-stage MDSC has been identified (*10*).

[1]Division of Hematology-Oncology, Beth Israel Deaconess Medical Center, Harvard Medical School, Boston, MA 02215, USA. [2]Department of Medicine, Beth Israel Deaconess Medical Center, Harvard Medical School, Boston, MA 02215, USA. [3]Cancer Center, Beth Israel Deaconess Medical Center, Harvard Medical School, Boston, MA 02215, USA.
*Present address: Heidelberg University, German Cancer Research Center (DKFZ), Heidelberg, Germany.
†Corresponding author. Email: vboussio@bidmc.harvard.edu

Although PMN-MDSCs represent the major subset of circulating MDSC, they are less immunosuppressive than M-MDSC when assessed on a per cell basis (*11*–*13*). Current views support the two-signal requirement for MDSC function. The first signal controls MDSC generation, whereas the second signal controls MDSC activation, which depends on cues provided by the TME and promotes MDSC differentiation to TAM (*14*). Proinflammatory cytokines and endoplasmic reticulum stress response in the TME contribute to pathologic myeloid cell activation that manifests as weak phagocytic activity, increased production of reactive oxygen species and nitric oxide (NO) and expression of arginase-1 (ARG1), and convert myeloid cells to MDSC (*9*). MDSCs are associated with poor outcomes in many cancer types in patients and negatively correlate with response to chemotherapy, immunotherapy, and cancer vaccines (*15*–*19*).

In the present study, we examined how PD-1 regulates the response of myeloid progenitors to cancer-driven emergency myelopoiesis and its implications on antitumor immunity. We determined that myeloid progenitors, which expand during cancer-driven emergency myelopoiesis, express PD-1 and PD-L1. PD-L1 was constitutively expressed on CMPs and GMPs, whereas PD-1 expression displayed a notable increase on GMPs that arose during tumor-driven emergency myelopoiesis. PD-1 was also expressed on tumor-infiltrating myeloid cells—including M-MDSCs and PMN-MDSCs, $CD11b^+F4/80^+$ MΦ, and $CD11c^+$major histocompatibility complex class II-positive ($MHCII^+$) dendritic cells (DCs) in tumor-bearing mice—and on MDSCs in patients with refractory lymphoma. Ablation of PD-1 signaling in PD-1 knockout (KO) mice prevented GMP accumulation and MDSC generation and resulted in increase of $Ly6C^{hi}$ effector monocytes, MΦ and DC. We generated mice with conditional targeting of the *Pdcd1* gene ($PD\text{-}1^{f/f}$) and selectively eliminated PD-1 in myeloid cells or T cells. Compared with T cell–specific ablation of PD-1, myeloid-specific PD-1 ablation more effectively decreased tumor growth in various tumor models. At a cellular level, only myeloid-specific PD-1 ablation skewed the myeloid cell fate commitment from MDSC to effector $Ly6C^{hi}$ monocytes MΦ and DC and induced T effector memory (T_{EM}) cells with improved functionality. Our findings reveal a previously unidentified role of the PD-1 pathway and suggest that skewing of myeloid cell fate during emergency myelopoiesis and differentiation to effector APCs, thereby reprogramming T cell responses, might be a key mechanism by which PD-1 blockade mediates antitumor function.

RESULTS

PD-1 is expressed in myeloid cells during cancer-mediated emergency myelopoiesis

For our studies, we selected the murine B16-F10 melanoma tumor model because it has been informative in dissecting mechanisms of resistance to checkpoint immunotherapy (*20*). First, we examined whether B16-F10 induces tumor-driven emergency myelopoiesis similarly to the MC17-51 fibrosarcoma, a mouse tumor model well established to induce cancer-driven emergency myelopoiesis (*21*). We assessed the expansion of myeloid progenitors in the bone marrow and the increase of $CD11b^+CD45^+$ myeloid cells in the spleen and tumor (figs. S1 and S2). Both tumor types induced increase of myeloid progenitors in the bone marrow and systemic increase of $CD45^+CD11b^+$ myeloid cells (fig. S3), providing evidence that B16-F10 melanoma is an appropriate tumor model to study tumor-driven emergency myelopoiesis and its consequences in tumor immunity. In the spleen of non–tumor-bearing mice, few myeloid cells constitutively expressed very low levels of PD-L1, whereas PD-1 was very low to undetectable (Fig. 1, A and B). In B16-F10 tumor-bearing mice, expression of PD-1 and PD-L1 was up-regulated on myeloid cells of the spleen (Fig. 1, C to F). PD-1 and PD-L1 were also expressed on myeloid cells at the tumor site (Fig. 1, G to I). All subsets of myeloid cells expanding in tumor-bearing mice including M-MDSCs, PMN-MDSCs, $CD11b^+F4/80^+$ MΦs, and $CD11c^+MHCII^+$ DCs expressed PD-1 (Fig. 1, D and G). Kinetics studies of PD-1 expression on myeloid cells in the spleen of tumor-bearing mice showed a gradual increase over time (Fig. 1, J to M).

Because myeloid cells that give rise to MDSC and TAM are generated from myeloid progenitors in the bone marrow during tumor-driven emergency myelopoiesis, we examined PD-1 and PD-L1 expression in these myeloid progenitors. In non–tumor-bearing mice, PD-1 was detected at very low levels on GMPs (Fig. 2A), whereas PD-L1 was constitutively expressed in CMPs but mostly on GMPs (Fig. 2B). In tumor-bearing mice, PD-L1 was up-regulated in CMPs and GMPs, and its expression levels remained elevated during all assessed time points (Fig. 2, F to J). PD-1 expression was induced on CMPs but more prominently on GMPs (Fig. 2, C to I). Kinetics studies showed that PD-1 expression on GMPs peaked early after tumor inoculation (Fig. 2, C, E, and I), at a time point when tumor growth was not yet measurable. Thus, induction of PD-1 expression in myeloid progenitors is an early event during tumor development.

To determine whether PD-1 expression on GMPs was mediated by growth factors regulating emergency myelopoiesis, we cultured bone marrow cells from non–tumor-bearing mice with granulocyte colony-stimulating factor (G-CSF), granulocyte-macrophage colony growth factor (GM-CSF), and the TLR4 ligand lipopolysaccharide. PD-1 that was constitutively expressed at low levels in GMPs was up-regulated by culture with each of these factors (fig. S4A), consistent with our findings that PD-1 expression was rapidly induced on GMPs of tumor-bearing mice in vivo (Fig. 2, C, E, and I). Quantitative polymerase chain reaction (qPCR) in purified Lin^{neg} bone marrow cells showed that PD-1 mRNA was constitutively expressed in myeloid progenitors and was up-regulated by culture with G-CSF or GM-CSF (fig. S4B). Together, these in vivo and in vitro studies provide evidence that PD-1 expression on myeloid progenitors is regulated by a direct cell-intrinsic effect of factors driving cancer-mediated emergency myelopoiesis.

To examine whether PD-1 was expressed in MDSCs in humans, we used samples from healthy donors and patients with malignant non-Hodgkin's lymphoma (NHL) (figs. S5 and S6). A high level of PD-1–expressing M-MDSCs was detected in the peripheral blood of three patients with treatment-refractory NHL but not in two patients who responded to treatment or five healthy donors (fig. S6). These results show that PD-1 expression is detected in human MDSCs and serve as a paradigm, suggesting that PD-1 expression in MDSCs of patients with cancer might be a clinically relevant event.

PD-1 ablation alters emergency myelopoiesis and the profile of myeloid cell output

To examine whether PD-1 might have an active role in tumor-induced stress myelopoiesis, we used PD-1–deficient ($PD\text{-}1^{-/-}$) mice. PD-1 deletion, which resulted in decreased tumor growth (Fig. 3, A and B), substantially altered tumor-induced stress myelopoiesis (Fig. 3, C to E). Although accumulation of CMPs was comparable, accumulation of GMPs was significantly diminished in $PD\text{-}1^{-/-}$ mice (Fig. 3, C and D), indicating that GMPs might be a key target on which PD-1 mediated

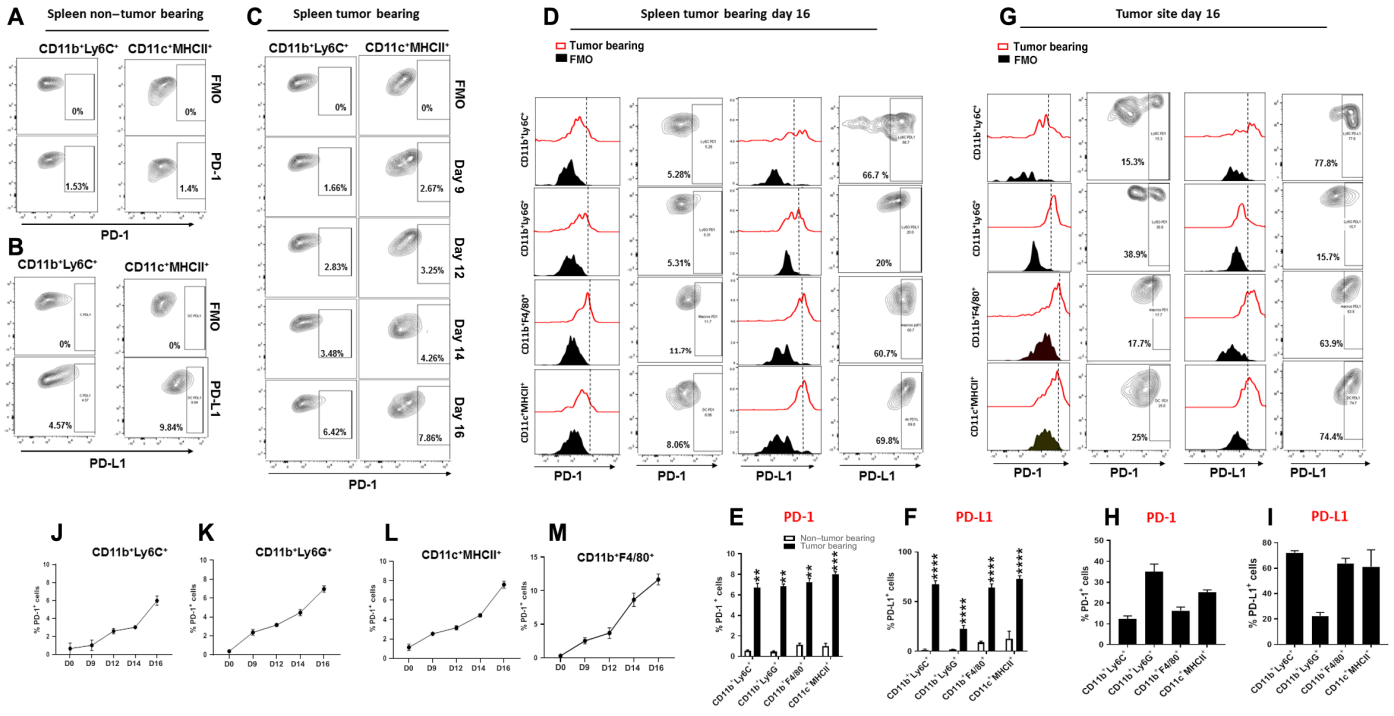

Fig. 1. PD-1 and PD-L1 are expressed on myeloid cells that expand in tumor-bearing mice. (**A** and **B**) Expression of PD-1 and PD-L1 on CD11b$^+$Ly6C$^+$ monocytes and CD11c$^+$MHCII$^+$ DC in the spleen of non–tumor-bearing C57BL/6 mice. FMO, fluorescence minus one. (**C**) C57BL/6 mice were inoculated with B16-F10 mouse melanoma, and at the indicated time points, expression of PD-1 was examined by flow cytometry in the spleen after gating on the indicated myeloid populations; contour plots depicting the percentage of positive cells are shown. On day 16 after tumor inoculation, expression of PD-1 and PD-L1 was assessed in the spleen (**D**) and the tumor site (**G**) after gating on the indicated myeloid populations. (D and G) Fluorescence-activated cell sorting (FACS) histograms and contour plots depicting the percentage of positive cells and bar graphs (**E**, **F**, **H**, and **I**) of mean ± SEM positive cells. Results are representative of 12 independent experiments with six mice per group. (**J** to **M**) Kinetics of PD-1 up-regulation on CD11b$^+$Ly6C$^+$, CD11b$^+$Ly6G$^+$, CD11b$^+$F4/80$^+$, and CD11c$^+$MHCII$^+$ of the spleen after tumor inoculation. $^{**}P < 0.01$, $^{***}P < 0.005$, $^{****}P < 0.001$.

its effects on myeloid progenitors (Fig. 3E). Kinetics studies showed sustained GMP expansion in wild-type (WT) tumor-bearing mice. In contrast, in PD-1$^{-/-}$ tumor-bearing mice, GMPs displayed a rapid expansion and subsequent decline (fig. S7). In parallel, in PD-1$^{-/-}$ mice, there was an increase of differentiated CD11b$^+$Ly6C^{hi} monocytic cells not only in the tumor (Fig. 3H) but also in the spleen and the small intestine, which also displayed an increase in CD11c$^+$MHCII$^+$ DCs (Fig. 3, F and G). Moreover, at these sites, there was a significant increase of the CD11b$^+$Ly6C$^+$/CD11b$^+$Ly6G$^+$ ratio (Fig. 3, I to K), indicating a shift of myelopoiesis output toward monocytic lineage dominance. These Ly6C^{hi} monocytes, CD11b$^+$F4/80$^+$ MΦs, and CD11c$^+$MHCII$^+$ DCs in PD-1$^{-/-}$ tumor-bearing mice expressed interferon (IFN) regulatory factor 8 (IRF8), and all myeloid subsets had elevated expression of the retinoic acid receptor-related orphan receptor γ (RORC or RORγ) (Fig. 3, L to N, and fig. S8). Similar results were observed in two additional tumor models, the MC38 colon adenocarcinoma and the MC17-51 fibrosarcoma model (fig. S9), both of which induced cancer-driven emergency myelopoiesis (fig. S3).

IRF8 regulates myeloid cell fate to monocyte/macrophage and DC differentiation versus granulocyte differentiation (*22*, *23*), explaining the increase of CD11b$^+$Ly6C$^+$/CD11b$^+$Ly6G$^+$ ratio that we observed in tumor-bearing PD-1 KO mice. IRF8 is designated as one of the "terminal selectors" that control the induction and maintenance of the terminally differentiated state of these myeloid cells (*22*, *23*). Moreover, IRF8 shifts the fate of myeloid cells away from immature MDSC, which are characterized by a restriction in IRF8 expression (*24*, *25*). Retinoid-related orphan nuclear receptors not only are required for myelopoiesis and are mediators of the inflammatory response of effector Ly6C^{hi} monocytes and macrophages (*21*, *26*) but also can be expressed by MDSC (*21*). For these reasons, we examined the functional properties of CD11b$^+$Ly6C$^+$ cells in PD-1$^{-/-}$ tumor-bearing mice. A key mechanism by which CD11b$^+$Ly6C$^+$ M-MDSCs mediate suppression of T cell responses involves the production of NO (*27*). We assessed the immunosuppressive function and found diminished NO production and diminished suppressor capacity of CD11b$^+$Ly6C$^+$ myeloid cells isolated from tumor-bearing PD-1$^{-/-}$ mice compared with their counterparts isolated from tumor-bearing WT control mice (Fig. 3, O and P). Thus, PD-1 ablation switches the fate and function of myeloid cells away from immunosuppressive MDSC and promotes the generation of differentiated monocytes, MΦ, and DC. The expansion of CD11b$^+$Ly6C^{hi} monocytes, the increase of the CD11b$^+$Ly6C$^+$/CD11b$^+$Ly6G$^+$ ratio, and the up-regulation of RORC in myeloid cells of the spleen of PD-1$^{-/-}$ mice were already observed on day 9 after tumor inoculation, when tumors were not yet measurable, and on day 12, when tumors in WT and PD-1$^{-/-}$ mice had comparable size (fig. S10). These results indicate that the effects of PD-1 ablation on the myeloid compartment of PD-1$^{-/-}$ tumor-bearing mice preceded the differences in tumor growth.

To determine the potential therapeutic relevance of these findings, we examined whether changes in the myeloid compartment might be detected during treatment with PD-1–blocking antibody. Compared

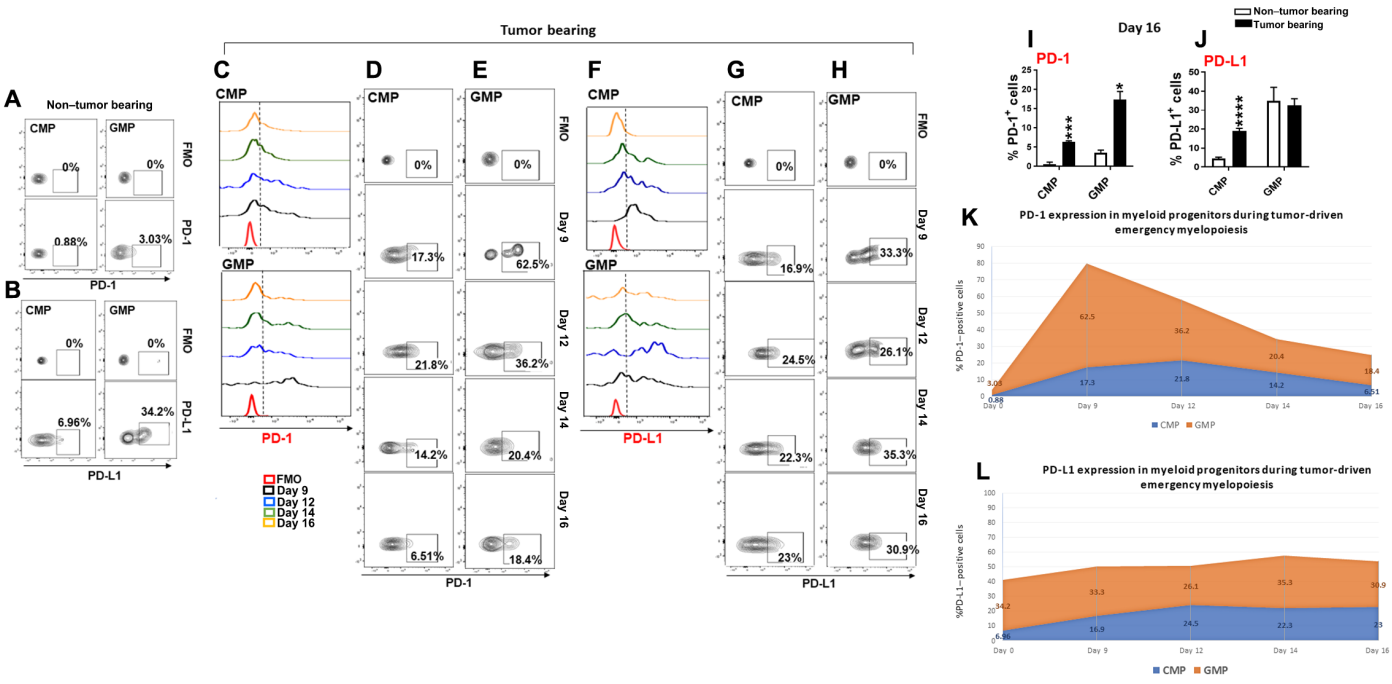

Fig. 2. PD-1 and PD-L1 are expressed on CMP and GMP myeloid progenitors during cancer-driven emergency myelopoiesis. (**A** and **B**) Expression of PD-1 and PD-L1 on CMPs and GMPs of non–tumor-bearing mice. (**C** to **J**) C57BL/6 mice were inoculated with B16-F10 mouse melanoma, and expression of PD-1 and PD-L1 on CMPs and GMPs was examined on days 9, 12, 14, and 16 after implantation. FACS histograms (C and F) and contour plots (D, E, G, and H) indicating the percentage of positive cells and bar graphs of mean ± SEM positive cells (I and J) are shown. Results are representative of four independent experiments with six mice per group. (**K** and **L**) Kinetics of PD-1 (K) and PD-L1 (L) expression on CMPs (blue) and GMPs (orange) during tumor-driven emergency myelopoiesis. Results are representative of four separate experiments with six mice per group. *$P < 0.05$, ***$P < 0.005$, ****$P < 0.001$.

with the control treatment group, mice receiving anti–PD-1 antibody (fig. S11A) had diminished accumulation of GMP in the bone marrow (fig. S11B) and increased expansion of Ly6C$^+$ monocytes and DC in the tumor site (fig. S11D), with effector features characterized by the expression of RORC, IRF8, and IFN-γ (fig. S11, E to G and I). In contrast, cells expressing interleukin-4 receptor α (IL-4Ra), a marker of MDSC (*10*, *28*), were significantly decreased (fig. S11H). Thus, treatment with anti–PD-1–blocking antibody promotes the differentiation of myeloid cells with effector features while suppressing expansion of MDSC in tumor-bearing mice.

Myeloid-specific PD-1 ablation is the key driver of antitumor immunity

To determine whether these changes on myeloid cell fate in PD-1$^{-/-}$ mice were mediated by myeloid cell–intrinsic effects of PD-1 ablation or by the effects of PD-1^{neg} T cells on myeloid cells, we generated mice with conditional targeting of *Pdcd1* gene (PD-1$^{f/f}$) (fig. S12A) and crossed them with mice expressing cre recombinase under the control of the lysozyme (LysM) promoter to induce selective ablation of the *Pdcd1* gene in myeloid cells (PD-1$^{f/fLysMcre}$) or with mice expressing cre recombinase under the control of the CD4 promoter to induce selective ablation of the *Pdcd1* gene in T cells (PD-1$^{f/fCD4cre}$) (fig. S12, B and C). In PD-1$^{f/fLysMcre}$ mice, tumor growth was significantly diminished (Fig. 4, A and B), indicating that despite the preserved PD-1 expression in T cells, myeloid-specific PD-1 ablation in PD-1$^{f/fLysMcre}$ mice was sufficient to inhibit tumor growth. Tumor-driven emergency myelopoiesis was selectively affected in PD-1$^{f/fLysMcre}$ mice. Although myeloid-specific PD-1 ablation resulted in expansion of CMPs, accumulation of GMPs was prevented (Fig. 4C). In contrast, no change on cancer-driven emergency myelopoiesis was detected in PD-1$^{f/fCD4cre}$ mice, which had comparable expansion of CMP and GMP to PD-1$^{f/f}$ control mice (Fig. 5A).

Myeloid-specific PD-1 ablation in PD-1$^{f/fLysMcre}$ mice not only shifted the differentiation of CD11b$^+$Ly6C$^+$ and CD11b$^+$Ly6G$^+$ myeloid subsets and increased the CD11b$^+$Ly6C$^+$/CD11b$^+$Ly6G$^+$ ratio in the spleen and tumor site as in PD-1$^{-/-}$ mice (Fig. 4, D to F) but also resulted in a notably different immunological profile of CD11b$^+$Ly6C$^+$ monocytic myeloid cells, consistent with effector myeloid function as indicated by the expression of effector myeloid cell markers including CD80, CD86, CD16/32 (Fc receptor II/III), and CD88 (C5aR) (Fig. 4G). Consistent with the improved function of myeloid cells, PD-1$^{f/fLysMcre}$ mice also had higher levels of IFN-γ–expressing CD11b$^+$Ly6C^{hi} monocytes and CD11b$^+$F4/80$^+$ MΦs (Fig. 4G and fig. S13, A and B) and increase of IRF8$^+$ and RORC$^+$ CD11b$^+$Ly6C^{hi} monocytes (fig. S13, C and D). In contrast, cells expressing IL-4Ra, CD206, and ARG1—which are markers of MDSC, immunosuppressive neutrophils, and tolerogenic DCs (*29*–*33*)—were diminished (Fig. 4, H and I). Thus, myeloid-intrinsic PD-1 ablation skews the fate of myeloid cells away from immunosuppressive MDSCs; promotes the differentiation of functional effector monocytes, MΦs, and DCs; and has a decisive role in systemic antitumor immunity despite PD-1 expression in T cells.

We studied antitumor responses in mice with T cell–specific PD-1 ablation and found that PD-1$^{f/fCD4cre}$ mice had diminished antitumor protection (Fig. 5, B and C). Consistent with the causative role of myeloid cell–specific PD-1 targeting in the differentiation and function

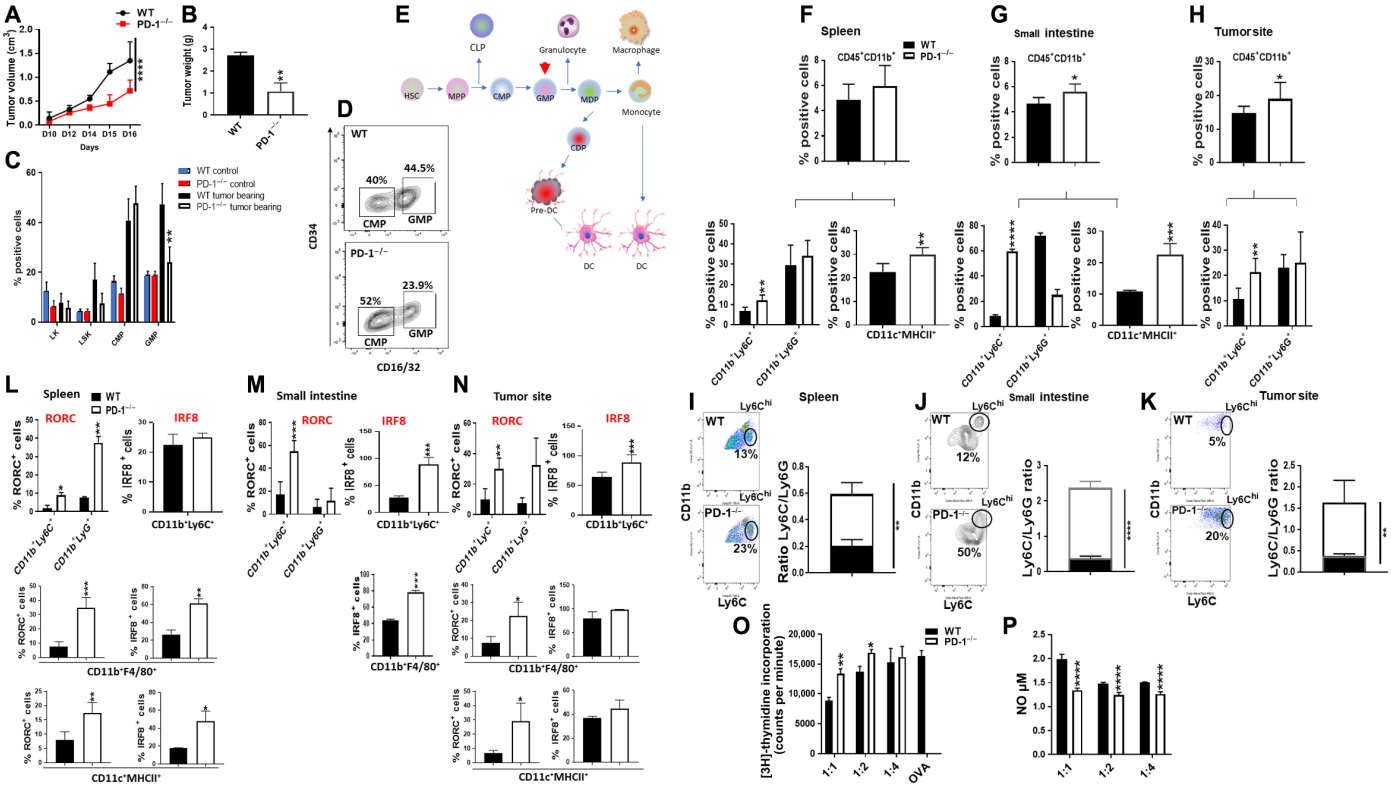

Fig. 3. PD-1 ablation alters emergency myelopoiesis and the profile of myeloid cell output. (**A** and **B**) WT and PD-1$^{-/-}$ mice were inoculated with B16-F10 melanoma, and tumor size was monitored daily (A). Mice were euthanized on day 16, and tumor weight was measured (B). Data shown are means ± SEM of six mice per group and are representative of six independent experiments. (**C**) Mean percentages ± SEM of LSK (Lin^{neg}, Sca1^{pos}, CD127^{neg}, c-kit^{pos}) and LK (Lin^{neg}, Sca1^{neg}, CD127^{neg}, c-kit^{pos}) hematopoietic precursors, CMP, and GMP in the bone marrow of non–tumor-bearing and tumor-bearing WT and PD-1$^{-/-}$ mice. GMPs in PD-1$^{-/-}$ mice were significantly lower compared with GMPs in WT mice (**$P < 0.01$). (**D**) Representative contour plots of FACS analysis for CMP and GMP in the bone marrow of tumor-bearing WT and PD-1$^{-/-}$ mice. (**E**) Schematic presentation of myeloid lineage differentiation. The arrowhead indicates GMP, the key target population of PD-1 during emergency myelopoiesis. HSC, hematopoietic stem cells; MPP, multi-potent progenitor; MDP, monocyte/macrophages and DC precursors; CDP, common dendritic cell progenitors; CLP, common lymphoid progenitors. (**F** to **H**) Mean percentages of CD45$^+$CD11b$^+$, CD11b$^+$Ly6C$^+$, CD11b$^+$Ly6G$^+$, and CD11c$^+$MHCII$^+$ in the spleen (F), small intestine (G), and B16-F10 site (H) of tumor-bearing WT and PD-1$^{-/-}$ mice. (**I** to **K**) Representative plots of FACS analysis for CD11b$^+$Ly6C^{hi} and CD11b$^+$Ly6C$^+$/CD11b$^+$Ly6G$^+$ ratio in the spleen (I), small intestine (J), and B16-F10 site (K). (**L** to **N**) Mean percentages ± SEM of RORC and IRF8 expressing CD11b$^+$Ly6C$^+$, CD11b$^+$Ly6G$^+$, CD11b$^+$F4/80$^+$, and CD11c$^+$MHCII$^+$ myeloid cells within the CD45$^+$CD11b$^+$ gate in the spleen (L), small intestine (M), and B16-F10 site (N). Data from one representative experiment of three independent experiments with six mice per group are shown. (**O** and **P**) Diminished suppressive activity (O) and NO production (P) of CD11b$^+$Ly6C$^+$ cells isolated from PD-1$^{-/-}$ tumor-bearing mice. CD11b$^+$Ly6C$^+$ cells were isolated from tumor-bearing WT and PD-1$^{-/-}$ mice and cultured at various ratios with OTI splenocytes stimulated with OVA$_{257–264}$. Data show means ± SEM of one representative of two experiments (*$P < 0.05$, **$P < 0.01$, ***$P < 0.001$, and ****$P < 0.001$).

of myeloid cells, T cell–specific PD-1 ablation did not induce expansion of CD11b$^+$CD45$^+$ leukocytes, CD11b$^+$F4/80$^+$ MΦs, and CD11c$^+$MHCII$^+$ DCs and increase of CD11b$^+$Ly6C$^+$/CD11b$^+$Ly6G$^+$ ratio (Fig. 5, D and E) or immunological features of functional effector myeloid cells (Fig. 5F) in PD-1$^{f/fCD4cre}$ tumor-bearing mice, compared with control tumor-bearing mice. Moreover, despite PD-1 ablation, tumor-bearing PD-1$^{f/fCD4cre}$ mice did not have quantitative differences in tumor-infiltrating T_{EM} cells compared with control tumor-bearing mice (Fig. 5G) or features of enhanced effector function as determined by assessment of cytokine-producing cells (Fig. 5, H to M).

Similar outcomes to those observed with B16-F10 tumor in the differentiation of myeloid cells toward myeloid effectors versus MDSC were obtained when PD-1$^{f/fLysMcre}$ and PD-1$^{f/fCD4cre}$ mice were inoculated with MC38 colon adenocarcinoma cells (Fig. 6, B to I). Moreover, PD-1$^{f/fLysMcre}$ but not PD-1$^{f/f\,CD4cre}$ mice inoculated with MC38 had functional differences in tumor-infiltrating T_{EM} and T central memory (T_{CM}) cells compared with control tumor-bearing mice (Fig. 6, J to L). In the context of this highly immunogenic tumor, PD-1 ablation in myeloid cells resulted in complete tumor eradication, whereas mice with PD-1 ablation in T cells showed progressive tumor growth (Fig. 6A). Together, these results suggest that by preventing the differentiation of effector myeloid cells and promoting generation of MDSC, myeloid-specific PD-1 expression has a decisive role on T cell function. Thus, although PD-1 is an inhibitor of T cell responses (*2*, *34*, *35*), ablation of PD-1 signaling in myeloid cells is an indispensable requirement for induction of systemic antitumor immunity in vivo.

To further investigate the direct effects of PD-1 on myeloid cell fate in the absence of T cells, we used recombination activating gene 2 (RAG2) KO mice (lacking mature T cells and B cells). Treatment of RAG2 KO tumor-bearing mice with anti–PD-1–blocking antibody resulted in decreased accumulation of GMPs during tumor-driven emergency myelopoiesis (fig. S14A), myeloid cell expansion in the spleen and tumor site (fig. S14, B and C), and enhanced generation of effector myeloid cells (fig. S14, D to G), providing evidence that blockade of PD-1–mediated signals skews myeloid lineage fate to

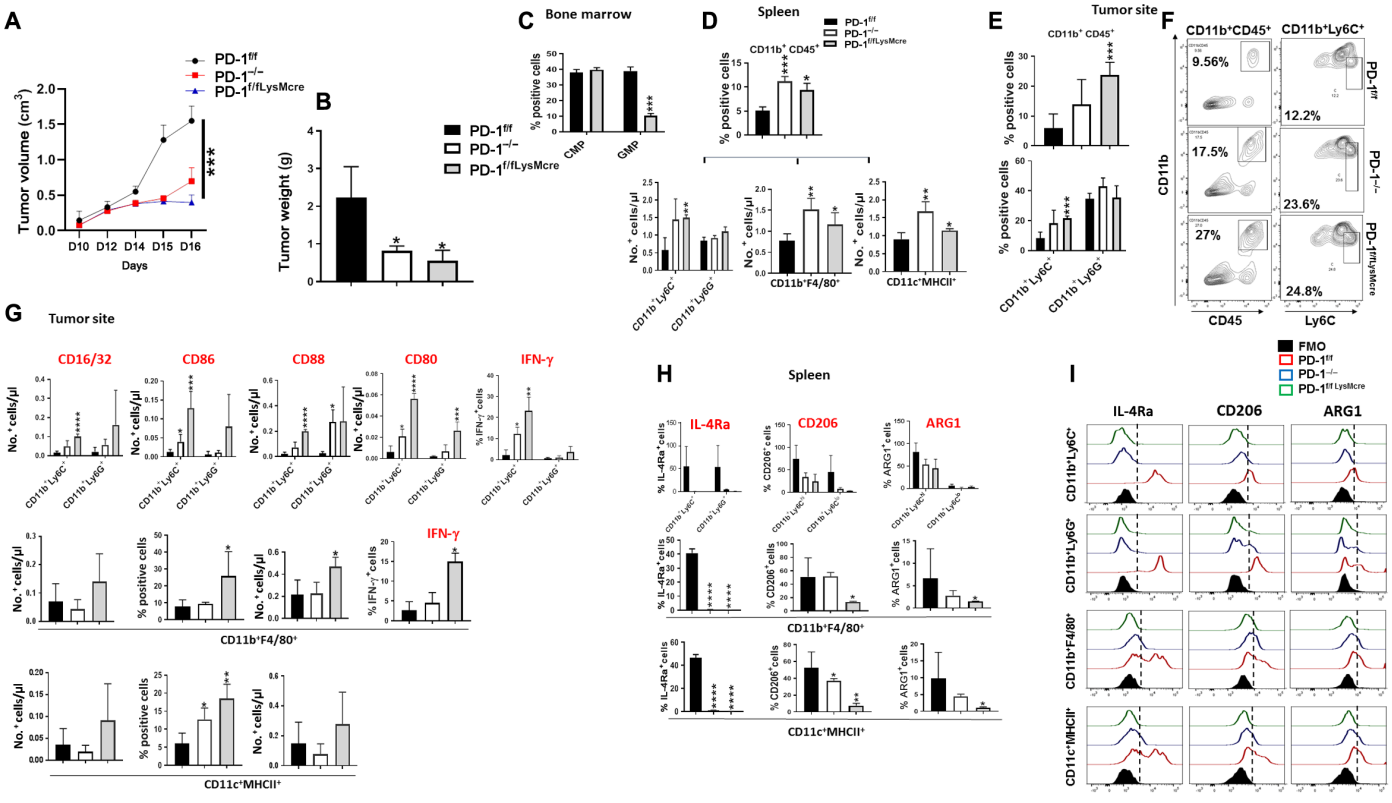

Fig. 4. Myeloid-specific PD-1 ablation is the driver of altered tumor-driven emergency myelopoiesis, inflammatory myeloid cell differentiation, and antitumor immunity. (**A** and **B**) PD-1$^{f/f}$, PD-1$^{f/fLysMcre}$, and PD-1$^{-/-}$ mice were inoculated with B16-F10 melanoma, and tumor size was monitored daily (A). After mice were euthanized, tumor weight was measured (B). (**C**) Mean percentages ± SEM of CMP and GMP in the bone marrow of tumor-bearing PD-1$^{f/f}$ and PD-1$^{f/fLysMcre}$ mice. (**D**) Mean percentages ± SEM of CD11b$^+$CD45$^+$ cells and CD11b$^+$Ly6C$^+$, CD11b$^+$Ly6G$^+$, CD11b$^+$F4/80$^+$, and CD11c$^+$MHCII$^+$ myeloid subsets in the spleen of tumor-bearing mice. (**E**) Mean percentages ± SEM of CD11b$^+$CD45$^+$, CD11b$^+$Ly6C$^+$, and CD11b$^+$Ly6G$^+$ cells and (**F**) representative contour plots of FACS analysis for CD11b$^+$CD45$^+$ and CD11b$^+$Ly6C$^+$ cells at the tumor site in PD-1$^{f/f}$, PD-1$^{f/fLysMcre}$, and PD-1$^{-/-}$ mice. (**G**) Mean percentages ± SEM of CD16/CD32$^+$, CD86$^+$, CD88$^+$, and CD80$^+$ cells and IFN-γ–expressing myeloid cell subsets within the CD45$^+$CD11b$^+$ gate in B16-F10 tumors from PD-1$^{f/f}$, PD-1$^{f/fLysMcre}$, and PD-1$^{-/-}$ mice. (**H**) Mean percentages ± SEM and (**I**) FACS histograms of IL-4Ra, CD206, and ARG1 expression in CD11b$^+$Ly6C$^+$, CD11b$^+$Ly6G$^+$, CD11b$^+$F4/80$^+$, and CD11c$^+$MHCII$^+$ myeloid cells within the CD11b$^+$CD45$^+$ gate in the spleen of tumor-bearing PD-1$^{f/f}$, PD-1$^{f/fLysMcre}$, and PD-1$^{-/-}$ mice. Data are from one representative of three independent experiments with six mice per group are shown in all the panels (*P < 0.05, **P < 0.01, ***P < 0.005, and ****P < 0.001).

myeloid effector cells in a myeloid cell–intrinsic and T cell–independent manner. In RAG2 KO mice treated with anti–PD-1 antibody, despite the absence of T cells, a decrease of tumor growth was also observed (fig. S14, H and I), suggesting that ablation of PD-1 signaling promotes myeloid-specific mechanisms that induce tumor suppression, one of which might involve increased phagocytosis (*8*).

PD-1 ablation alters the signaling responses of myeloid cells to factors of emergency myelopoiesis

To understand mechanisms that might be responsible for the significant differences of myeloid cell fate commitment induced by myeloid-specific PD-1 targeting, we examined whether PD-1–deficient bone marrow myeloid progenitors might have distinct signaling responses to the key hematopoietic growth factors that mediate cancer-driven emergency myelopoiesis, which also induced PD-1 expression in GMP during in vitro culture. To avoid any potential impact of bone marrow–residing PD-1$^{-/-}$ T cells or mature myeloid cells on the signaling responses of myeloid progenitors, we used Lin^{neg} bone marrow from PD-1$^{f/fLysMcre\ mice}$ because LysMcre is expressed in CMPs and GMPs (*36*), allowing us to take advantage of the selective deletion of PD-1 in these myeloid progenitors. PD-1–deficient GMPs (fig. S15) had enhanced activation of extracellular signal–regulated kinase 1/2 (Erk1/2), mammalian target of rapamycin complex 1 (mTORC1), and signal transducer and activator of transcription 1 (STAT1) in response to G-CSF, a main mediator of emergency myelopoiesis (*37*, *38*). These results are notable because each of these signaling targets has a decisive role in the differentiation and maturation of myeloid cells while preventing the generation of immature immunosuppressive MDSC (*39*–*42*). These findings indicate that PD-1 might affect the differentiation of myeloid cells by regulating the fine tuning of signaling responses of myeloid progenitors to hematopoietic growth factors that induce myeloid cell differentiation and lineage fate determination during emergency myelopoiesis.

PD-1 ablation alters the metabolic program of myeloid progenitors and activates cholesterol synthesis

Metabolism has a decisive role in the fate of hematopoietic and myeloid precursors. Stemness and pluripotency are regulated by maintenance of glycolysis (*43*). Switch from glycolysis to mitochondrial metabolism and activation of oxidative phosphorylation and trichloroacetic acid (TCA) cycle are associated with differentiation (*44*). This is initiated by glycolysis-mediated mitochondrial biogenesis

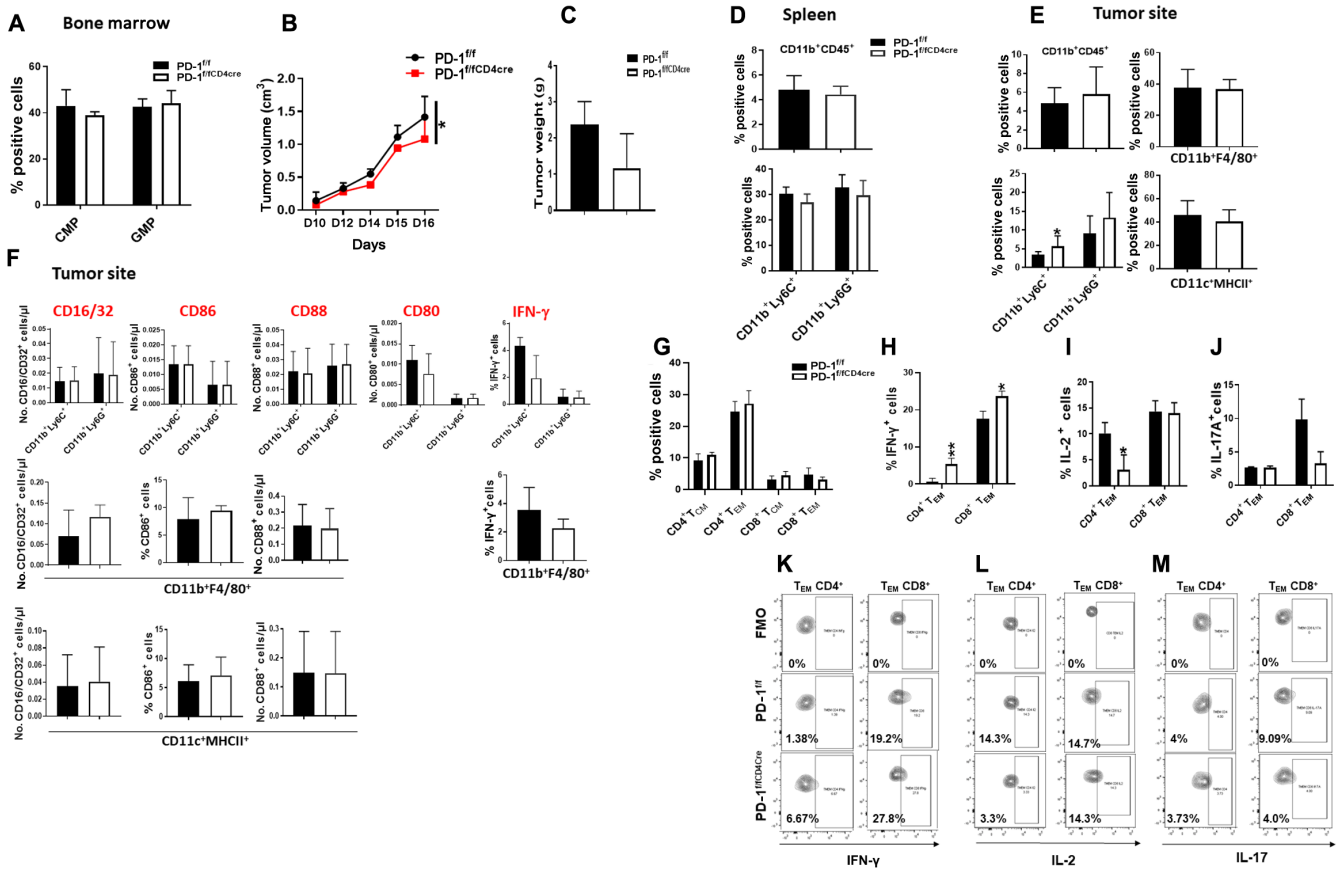

Fig. 5. T cell–specific PD-1 ablation has no impact on tumor-driven emergency myelopoiesis and the profile of myeloid cell output and provides minimal protection against tumor growth. PD-$1^{f/f}$ and PD-$1^{f/fCD4cre}$ mice were inoculated with B16-F10 melanoma. (**A**) On day 16, mice were euthanized, and bone marrow CMPs and GMPs were examined by flow cytometry. Mean percentages ± SEM of CMP or GMP are shown. (**B** and **C**) Tumor size was assessed every other day from inoculation (B). On the day of euthanasia, tumor weight was measured (C). (**D**) Mean percentages ± SEM of $CD11b^+CD45^+$ cells and $CD11b^+Ly6C^+$ and $CD11b^+Ly6G^+$ populations within the $CD11^+CD45^+$ gate in the spleen. (**E**) Mean percentages ± SEM of $CD11b^+CD45^+$ cells and $CD11b^+Ly6C^+$, $CD11b^+Ly6G^+$, $CD11b^+F4/80^+$, and $CD11c^+MHCII^+$ cells within the $CD11b^+CD45^+$ gate in the tumor site. (**F**) Mean percentages ± SEM of CD16/$CD32^+$, $CD86^+$, $CD88^+$, $CD80^+$, and IFN-γ expression in the indicated myeloid subsets ($CD11b^+Ly6C^+$, $CD11b^+Ly6G^+$, $CD11b^+F4/80^+$, and $CD11c^+MHCII^+$) within the $CD11b^+CD45^+$ gate in the tumor site. (**G** to **J**) Mean percentages ± SEM of $CD4^+$ and $CD8^+$ T_{CM} and T_{EM} (G), as well as IFN-γ, IL-2, and IL-17 (H to J) expression in $CD4^+$ and $CD8^+$ T_{EM} and T_{CM} at the tumor site, and respective contour plots (**K** to **M**). Results are from one representative of two independent experiments with six mice per group are shown (*$P < 0.05$ and **$P < 0.01$).

and epigenetic regulation of gene expression (*43*). The structural remodeling of the mitochondrial architecture during differentiation is characterized by increased replication of mitochondrial DNA to support production of TCA cycle enzymes and electron transport chain subunits, linking mitochondrial metabolism to differentiation (*45*).

We examined whether PD-1 ablation, which promoted the differentiation of myeloid cells in response to tumor-mediated emergency myelopoiesis, might affect the metabolic properties of myeloid precursors. Lin^{neg} bone marrow myeloid precursors were cultured with the cytokines G-CSF/GM-CSF/IL-6 that drive tumor-mediated emergency myelopoiesis in cocktail (Fig. 7, A and B) or individually (Fig. 7, C and D). Hematopoietic stem cell differentiation was documented by decrease of Lin^{neg}, which was more prominent in the cultures of PD-1–deficient bone marrow cells, and coincided with increase of $CD45^+CD11b^+$ cells (Fig. 7, A and B). $Ly6C^+$ monocytic cells dominated in the PD-$1^{f/fLysMcre}$ cultures, whereas $Ly6G^+$ granulocytes were decreasing compared with PD-$1^{f/f}$ control cultures (Fig. 7, C and D), providing evidence for a cell-intrinsic mechanism of PD-1–deficient myeloid precursors for monocytic lineage commitment. Glucose uptake, but more prominently, mitochondrial biogenesis, was elevated in PD-1–deficient CMP and GMP (Fig. 7, E and F). Bioenergetics studies showed that PD-1–deficient cells developed robust mitochondrial activity (Fig. 7G) and increase of oxygen consumption rate (OCR)/extracellular acidification rate (ECAR) ratio during culture (Fig. 7H), indicating that mitochondrial metabolism progressively dominated over glycolysis. This bioenergetic profile is consistent with metabolism-driven enhanced differentiation of hematopoietic and myeloid precursors (*45*, *46*).

We performed unbiased global metabolite analysis to determine whether PD-1–deficient myeloid precursors developed a distinct metabolic program. Compared with control, PD-1–deficient cells had elevated metabolic intermediates of glycolysis and pentose phosphate pathway (PPP), acetyl–coenzyme A (coA), and the TCA cycle metabolites citrate and α-ketoglutarate, but the most prominent difference was the elevated cholesterol (Fig. 7I, figs. S16 and S17, and table S1). Abundant cytosolic acetyl-coA can be used for fatty acid and cholesterol biosynthesis (fig. S17) (*43*). Moreover, mTORC1 activates de novo cholesterol synthesis via sterol regulatory element-binding

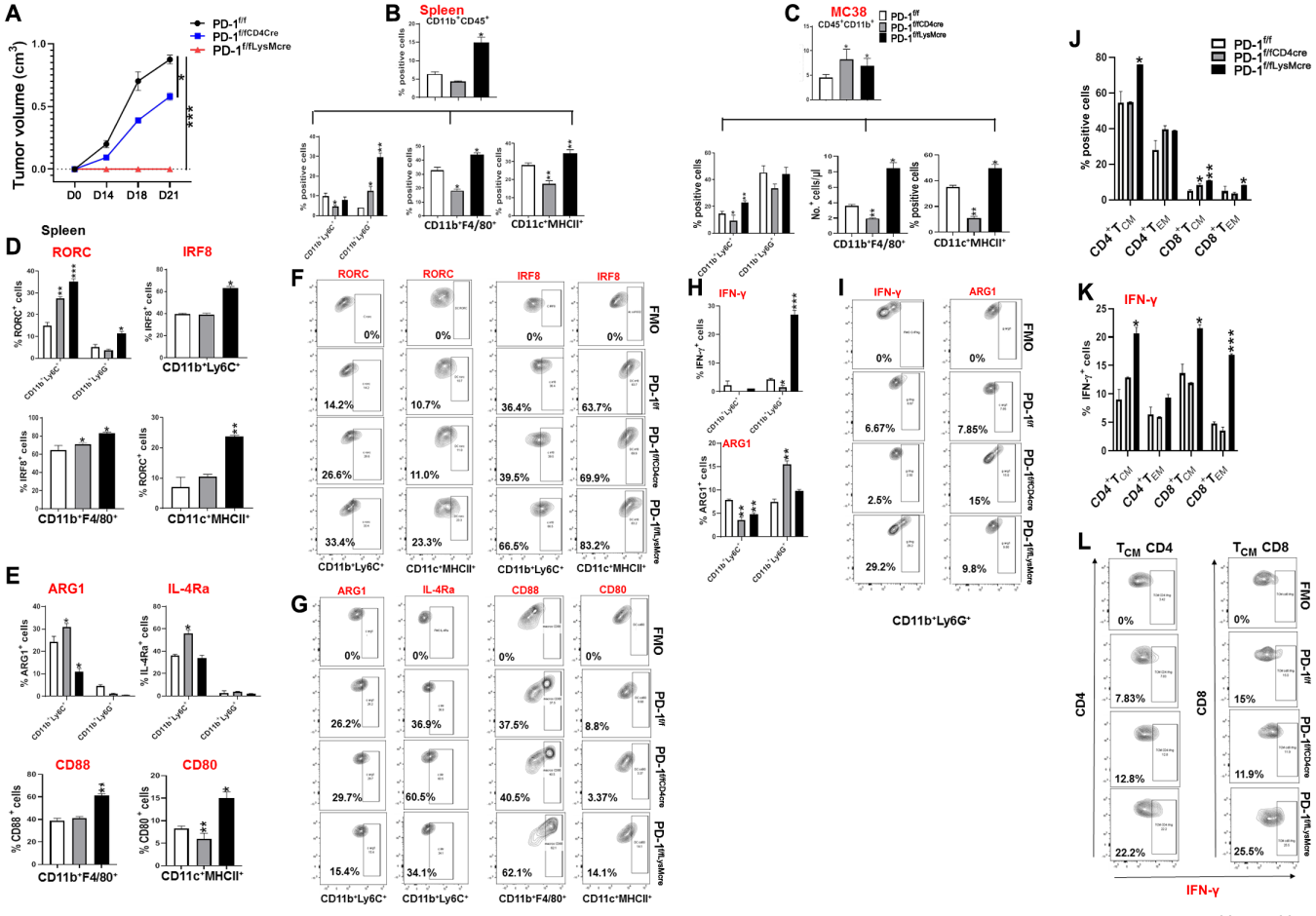

Fig. 6. T cell–specific PD-1 ablation provides diminished protection against tumor growth compared with myeloid-specific PD-1 ablation. (**A**) PD-1$^{f/f}$, PD-1$^{f/fCD4cre}$, and PD-1$^{f/fLysMcre}$ mice were inoculated with MC38 colon adenocarcinoma, and tumor size was monitored daily. Mice were euthanized on day 21, and mean percentages ± SEM of CD45$^+$CD11b$^+$ cells and CD11b$^+$Ly6C$^+$, CD11b$^+$Ly6G$^+$, CD11b$^+$F4/80$^+$, and CD11c$^+$MHCII$^+$ myeloid subsets in the spleen (**B**) and tumor site (**C**) were determined. (**D**) Mean percentages ± SEM of RORC- and IRF8-expressing CD11b$^+$Ly6C$^+$, CD11b$^+$Ly6G$^+$, CD11b$^+$F/480$^+$, and CD11c$^+$MHCII$^+$ myeloid cells and (**E**) mean percentages ± SEM of ARG1, IL-4Ra, CD88, and CD80 cells within the same myeloid subsets in the spleen. (**F** and **G**) Representative flow cytometry plots for RORC and IRF8 expression. (**H**) Mean percentages ± SEM and (**I**) representative flow cytometry plots of IFN-γ– and ARG1-expressing CD11b$^+$Ly6C$^+$ and CD11b$^+$Ly6G$^+$ myeloid cells at the tumor site. (**J** to **L**) Mean percentages ± SEM of CD4$^+$ and CD8$^+$ T_{CM} and T_{EM} cells (J) and IFN-γ–expressing CD4$^+$ and CD8$^+$ T_{EM} and T_{CM} at the tumor site (K) and respective contour plots (L). Data are from one representative of three experiments with six mice per group (*$P < 0.05$, **$P < 0.01$, and ***$P < 0.001$).

protein 1 (SREBP1), which regulates transcription of enzymes involved in cholesterol synthesis (*47*, *48*). Because acetyl-coA was elevated (Fig. 7I and fig. S17) and mTORC1 activation was enhanced in PD-1–deficient myeloid progenitors in response to growth factors driving emergency myelopoiesis (fig. S15), we examined whether activation of the mevalonate pathway that induces cholesterol synthesis (fig. S18A) might be involved. In PD-1–deficient myeloid progenitors cultured with growth factors of emergency myelopoiesis, mRNA of genes regulating cholesterol synthesis and uptake was increased, mRNA of genes promoting cholesterol metabolism was decreased (Fig. 7J and fig. S18B), whereas cellular cholesterol and neutral lipid content was elevated (Fig. 7, K to M). PD-1–deficient DC not only differentiated in vitro in the presence of B16-F10 tumor supernatant but also had a significant increase of cholesterol and neutral lipids compared with similarly differentiated DC from control mice (Fig. 7N). Consistent with these in vitro findings, glucose uptake and content of cholesterol and neutral lipids were elevated in GMPs of tumor-bearing PD-1 KO mice compared with control mice at days 7 or 9 after tumor inoculation, respectively, when tumors were not yet detectable or tumors in WT and PD-1 mice had equal size (fig. S19). Thus, features associated with metabolism-driven differentiation of myeloid progenitors are enhanced early in tumor-bearing PD-1 KO mice.

In addition to cholesterol synthesis, mevalonate also leads to the synthesis of isoprenoids, including geranylgeranyl pyrophosphate (GGPP) (fig. S17), which is required for protein geranylgeranylation catalyzed by geranylgeranyltransferase and has an active role in the up-regulation of RORC expression (*49*). Our metabolite analysis showed increased GGPP (Fig. 7I), providing a mechanistic explanation for the up-regulation of RORC in PD-1–deficient myeloid cells. Cholesterol accumulation is associated with skewing of hematopoiesis toward myeloid lineage and monocytosis, induces a proinflammatory program in monocytes/macrophages and DC, and amplifies TLR signaling (*50*–*52*). Together, these results unravel a previously unidentified role of PD-1 targeting in regulating myeloid lineage fate commitment and proinflammatory differentiation of monocytes,

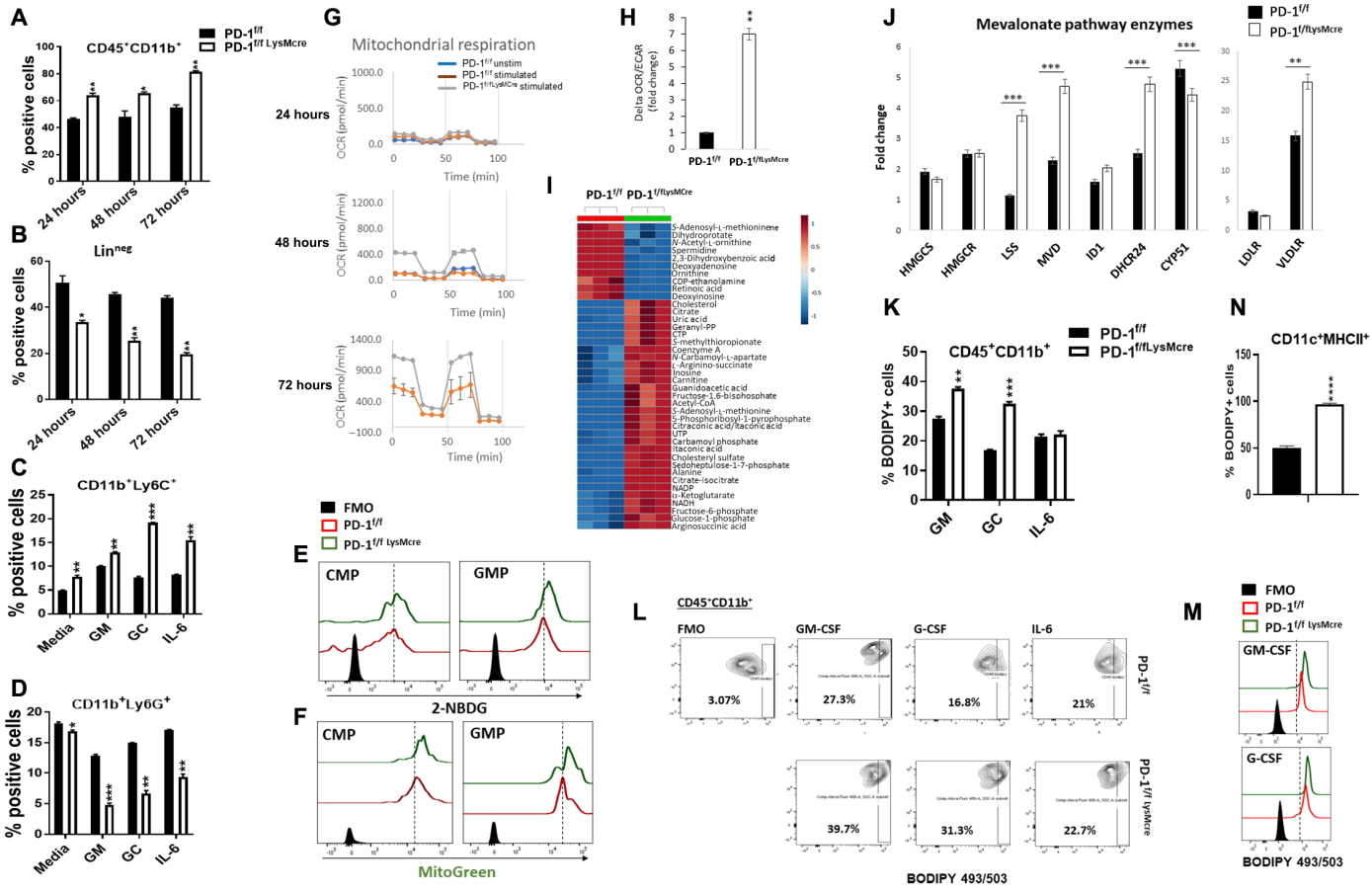

Fig. 7. Myeloid-specific PD-1 ablation reprograms myeloid cell signaling and metabolism and induces cholesterol synthesis. (**A** and **B**) Lin^{neg} bone marrow from PD-1$^{f/f}$ and PD-1$^{f/fLysMcre}$ mice was cultured with GM-CSF, G-CSF, and IL-6 for the indicated time intervals. Mean percentages ± SEM of CD11b^{+}CD45^{+} (A) and Lin^{neg} cells (B) are shown. (**C** and **D**) Bone marrow cells purified as in (A) and (B) were cultured with the indicated growth factors, and mean percentages ± SEM of CD11b^{+}Ly6C^{+} and CD11b^{+}Ly6G^{+} cells were examined after 48 hours of culture. (**E** to **H**) Bone marrow cells were prepared and cultured as in (A) and (B), and at 48 hours of culture, glucose uptake was assessed using 2-[N-(7-Nitrobenz-2-oxa-1,3-diazol-4-yl)Amino]-2-Deoxyglucose (2-NBDG) (E), and mitochondrial biogenesis was assessed by MitoGreen staining and flow cytometry (F). (G) At 24, 48, and 72 hours of culture, OCR and ECAR were measured by a Seahorse extracellular flux analyzer, and mitostress responses at each time point of culture were examined. (H) OCR/ECAR ratio was measured at these time points, and the increase of OCR/ECAR ratio during stimulation was calculated. (**I**) Lin^{neg} bone marrow cells from PD-1$^{f/f}$ and PD-1$^{f/fLysMcre}$ mice were cultured with G-CSF and GM-CSF for 48 hours, and metabolite analysis was performed by mass spectrometry. The unsupervised hierarchical clustering heat map of the top 50 metabolites is shown. (**J**) At 24, 48, and 72 hours of culture with G-CSF and GM-CSF, mRNA was extracted and analyzed for the expression of the indicated genes by qPCR. Results of the 48-hour culture are shown and are presented as the fold increase over the mRNA level expressed by PD-1$^{f/f}$ cells. Results are from one of three independent experiments. (**K** to **M**) At 24 hours of culture with GM-CSF, G-CSF, or IL-6, the content of neutral lipid droplets, including triglycerides and cholesterol esters, was assessed by flow cytometry using boron-dipyrromethene (BODIPY) 493/503. Mean percentages ± SEM (K) of BODIPY 493/503–positive cells within the CD11b^{+}CD45^{+} gate, representative contour plots (L), and histograms of FACS analysis (M) are shown. (**N**) PD-1$^{f/f}$ and PD-1$^{f/fLysMcre}$ DC were differentiated in the presence of B16-F10 tumor supernatant, and the content of neutral lipids was assessed. Mean percentage ± SEM of BODIPY 493/503–positive DC within the CD45^{+}CD11b^{+} gate is shown. Results are representative of three experiments. *P < 0.05, **P < 0.01, and ***P < 0.005.

macrophages, and DC during tumor-driven emergency myelopoiesis, through metabolic reprogramming.

Myeloid-specific PD-1 ablation induces improved T cell functionality

Previously, it was determined that monocyte/macrophage terminal differentiation is controlled by the combined actions of retinoid receptors and the nuclear receptor peroxisome proliferator–activated receptor γ (PPARγ), which is regulated by cholesterol and promotes gene expression and lipid metabolic processes, leading to terminal macrophage differentiation (*26*, *53*). Because our in vitro studies showed that PD-1–deficient myeloid progenitors developed a distinct metabolic program with elevated cholesterol metabolism, we examined whether PD-1 ablation might alter the expression of PPARγ in addition to RORC. We found that the expression of PPARγ was elevated in CD11b^{+}Ly6C^{+} monocytic cells and MΦ isolated from tumors of PD-1$^{-/-}$ and PD-1$^{f/fLysMcre}$ mice (Fig. 8, A to C). Because PD-1–deficient myeloid progenitors developed robust mitochondrial activity during culture in vitro (Fig. 7, G and H) and PPARγ is involved in mitochondrial function (*53*), we examined whether myeloid cells in tumor-bearing mice have improved mitochondrial metabolism, a feature that has an important role in supporting antitumor function of other immune cells (*54*). Monocytes, MΦ, and DC isolated from tumor of PD-1$^{-/-}$, and PD-1$^{f/fLysMcre}$ mice had increased mitochondrial

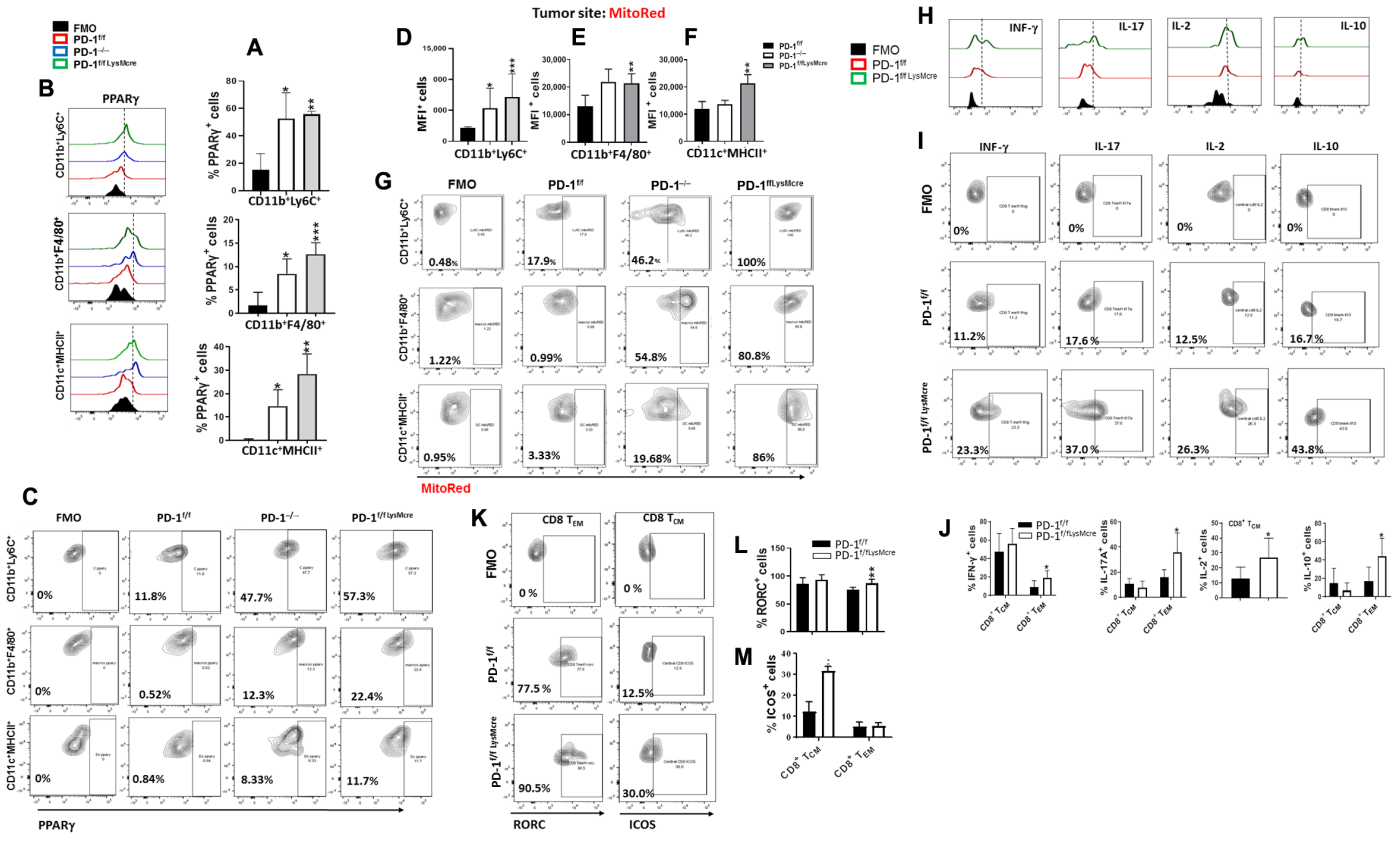

Fig. 8. PD-1 ablation induces enhanced mitochondrial metabolism of myeloid cells in tumor-bearing mice and improved T cell function. (**A** to **C**) Expression of PPARγ in myeloid cells at the B16-F10 site in PD-1$^{f/f}$, PD-1$^{f/fLysMcre}$, and PD-1$^{-/-}$ mice was examined by flow cytometry. Mean percentages ± SEM (A), representative histograms (B), and contour plots (C) of PPARγ-expressing CD11b$^+$Ly6C$^+$, CD11b$^+$F4/80$^+$, and CD11c$^+$MHCII$^+$ subsets. (**D** to **G**) Mitochondrial metabolic activity of myeloid cells at the B16-F10 tumor site in PD-1$^{f/f}$, PD-1$^{f/fLysMcre}$, and PD-1$^{-/-}$ mice was examined by assessing mitochondrial membrane potential using MitoRed. Mean fluorescence intensity (MFI) ± SEM of MitoRed–positive CD11b$^+$Ly6C$^+$, CD11b$^+$F4/80$^+$, and CD11c$^+$MHCII$^+$ subsets within the CD45$^+$CD11b$^+$ gate (D to F) and representative plots of FACS analysis (G) are shown. (**H** to **L**) In parallel, expression of IFN-γ, IL-17A, IL-2, IL-10, RORC, and ICOS in CD8$^+$ T_{CM} and T_{EM} isolated from B16-F10–bearing PD-1$^{f/f}$ and PD-1$^{f/fLysMcre}$ mice was assessed by flow cytometry. Representative histograms (H), contour plots (I and K), and mean percentages ± SEM (J, L, and **M**) within the CD44^{hi}CD62L^{hi} gate (for T_{CM}) and CD44^{hi}CD62^{lo} gate (for T_{EM}) cells are shown. Data are from one representative of four independent experiments (*P < 0.05, **P < 0.01, and ***P < 0.005).

membrane potential compared with myeloid cells from control tumor-bearing mice, consistent with enhanced mitochondrial metabolism (Fig. 8, D to G).

We investigated whether these significant immunometabolic changes of myeloid cells, induced by myeloid-specific PD-1 targeting, affected immunological properties of T cells that have key roles in their antitumor function. Compared with control PD-1$^{f/f}$ tumor-bearing mice, PD-1$^{f/fLysMcre}$ tumor-bearing mice had no quantitative differences in CD4$^+$ or CD8$^+$ T_{EM} and T_{CM} cells (fig. S20A) but had significant functional differences. There was an increase of IFN-γ–, IL-17–, and IL-10–producing CD8$^+$ T_{EM} cells and IL-2–producing CD8$^+$ T_{CM} cells (Fig. 8, H to J). Inducible T cell costimulator (ICOS) and lymphocyte-activation gene 3 (Lag3) were elevated in T cells from PD-1$^{f/fLysMcre}$ tumor-bearing mice but cytotoxic T-lymphocyte-associated protein 4 (CTLA4), T cell immunoglobulin and mucin domain 3 (Tim3), CD160, and PD-1/PD-L1 were comparable in T cells from PD-1$^{f/f}$ and PD-1$^{f/fLysMcre}$ tumor-bearing mice (Fig. 8, K to M, and fig. S20B). These findings are significant because IL-17–producing T helper cell 17 (T_H17)/ T cytotoxic cell 17 (Tc17) cells have enhanced antitumor function and mediate durable tumor growth inhibition (*55*). Moreover, T cells with a "hybrid" phenotype producing both IFN-γ and IL-17 might have superior antitumor properties by combining the enhanced effector function of T_H1/Tc1 and the longevity and stemness of T_H17/Tc17 cells (*56*). In our studies, these properties of T_{EM} cells correlated with improved antitumor function in PD-1$^{f/fLysMcre}$ mice.

To examine experimentally whether PD-1–deficient myeloid cells differentiated in tumor-bearing mice in vivo have improved capacity of inducing antigen-specific T cell responses, we assessed responses of the same primary CD4$^+$ or CD8$^+$ T cells to antigen-loaded DCs isolated from PD-1$^{-/-}$ or control mice bearing B16-F10 tumors (fig. S21A). DCs isolated from the spleen of tumor-bearing WT and PD-1$^{-/-}$ mice were pulsed with ovalbumin (OVA) and cocultured with OVA-specific CD4$^+$ or CD8$^+$ T cells from OTI or OTII T cell receptor (TCR)–transgenic mice. DCs from tumor-bearing PD-1$^{-/-}$ mice had superior ability to induce OTI and OTII T cell proliferation and IFN-γ expression (fig. S21, B and C). Together, our data provide evidence that myeloid cell–intrinsic PD-1 ablation induces potent antitumor immunity by decreasing accumulation of MDSC and promoting proinflammatory and effector monocytic/macrophage and DC differentiation, thereby leading to enhanced effector T cell responses.

DISCUSSION

Our present studies reveal a previously unidentified role of the PD-1 pathway in regulating lineage fate commitment and function of myeloid cells that arise from tumor-driven emergency myelopoiesis. These outcomes are mediated by myeloid-intrinsic effects of PD-1 ablation, leading to altered signaling and metabolic reprogramming of myeloid progenitors characterized by enhanced differentiation and elevated cholesterol synthesis. Consequently, the accumulation of immature immunosuppressive and tumor-promoting MDSC is diminished, and the output of differentiated, inflammatory effector monocytes, MΦ, and DC is enhanced. These immunometabolic changes of myeloid cells promote the differentiation of T_{EM} cells and systemic antitumor immunity in vivo despite preserved PD-1 expression in T cells.

We found that PD-1–deficient myeloid progenitors had enhanced activation of Erk1/2 and mTORC1 in response to G-CSF. These results indicate that Erk1/2 and mTORC1, a downstream mediator of phosphatidylinositol 3-kinase (PI3K)/Akt signaling, which are major targets of PD-1 in T cells (*2*), are subjected to PD-1–mediated inhibition in myeloid cells. These results are revealing because Erk1/2 phosphorylation subverts MDSC-mediated suppression by inducing M-MDSCs differentiation to APC (*39*). Erk and PI3K regulate glycolysis in response to G-CSF (*57*). PI3K/Akt/mTORC1 signaling is critical in myeloid lineage commitment. Expression of constitutively active Akt in $CD34^+$ cells induces enhanced monocyte and neutrophil development, whereas a dominant negative Akt has the opposite effect (*58*). mTORC1 is necessary for the transition of hematopoietic cells from a quiescent state to a prepared "alert" state in response to injury-induced systemic signals (*59*), for G-CSF–mediated differentiation of myeloid progenitors (*40*), and for M-CSF–mediated monocyte/macrophage generation (*41*). mTORC1 stimulates translation initiation through phosphorylation of 4E (eIF4E)–binding protein 1 (4E-BP1) and ribosomal S6 kinases and has a decisive role in the expression of glucose transporters and enzymes of glycolysis and PPP (*47*). Consistent with these, our studies showed that PD-1–deficient myeloid progenitors had elevated expression of glycolysis and PPP intermediates after culture with emergency cytokines in vitro and enhanced monocytic differentiation in tumor-bearing mice in vivo. Together, our findings indicate that PD-1 might affect the differentiation of myeloid cells by regulating the fine tuning of signaling responses of myeloid progenitors to hematopoietic growth factors that induce myeloid cell differentiation and lineage fate determination during emergency myelopoiesis. Further studies will identify how receptor-proximal signaling events mediated by hematopoietic growth factors are targeted by PD-1 in a manner comparable to PD-1–mediated targeting of signaling pathways in T cells (*2*, *34*, *35*).

Our metabolite analysis showed that a notable difference of PD-1–deficient myeloid progenitors was the increased expression of mevalonate metabolism enzymes and the elevated cholesterol. mTORC1 activates SREBP1, which induces transcription of enzymes involved in fatty acid and cholesterol synthesis (*48*), thereby leading to glycolysis-regulated activation of the mevalonate pathway. Our signaling studies showing enhanced mTORC1 activation and our metabolic studies showing enhanced mitochondrial metabolism and increased cholesterol content in PD-1–deficient myeloid cells provide a mechanistic link between the altered differentiation of PD-1–deficient myeloid progenitors and the altered immunophenotypic and functional program of PD-1–deficient monocytes, MΦ, and DC in tumor-bearing mice. Cholesterol drives myeloid cell expansion and differentiation of macrophages and DC (*50*, *51*, *60*) and promotes antigen-presenting function (*61*). These properties are consistent with the metabolic profile and the increased cholesterol of PD-1–deficient myeloid progenitors; the inflammatory and effector features of differentiated monocytes, MΦ, and DC; and the enhanced T effector cell activation in tumor-bearing mice with myeloid-specific PD-1 ablation that we identified in our studies. By such mechanism, PD-1 might centrally regulate antitumor immunity, independently of the expression of PD-1 and its ligands in the TME. Our studies showed that PD-1 expression on myeloid progenitors is an early event during tumor-mediated emergency myelopoiesis and indicate that PD-1 blockade at early stages of cancer might have a decisive effect on antitumor immunity by preventing MDSC generation from myeloid progenitors and inducing the systemic output of effector myeloid cells that drive antitumor T cell responses.

In addition to its expression in myeloid progenitors, in the bone marrow, we found that PD-1 is expressed in all myeloid subsets including M-MDSC, PMN-MDSC, $CD11b^+F4/80^+$ MΦ, and $CD11c^+MHCII^+$ DC in the tumor and the spleen of tumor-bearing mice, albeit at different levels. This difference might be related to gradient of tumor-derived factors responsible for PD-1 induction such as G-CSF and GM-CSF that we found to induce PD-1 transcription in myeloid progenitors. This possibility would be consistent with the gradual up-regulation of PD-1 expression in splenic myeloid cells, determined by our kinetics studies, which correlates with tumor growth that might be responsible for the increase of systemic levels of tumor-derived soluble factors that induce PD-1. Other cues of the TME known to mediate the activation step of MDSC (*14*) might also be responsible for the induction of higher PD-1 expression level in the tumor versus the splenic myeloid cells. Our findings unravel a previously unidentified role of PD-1 in myeloid cell fate commitment during emergency myelopoiesis, a process that is involved not only in antitumor immunity but also in the control of pathogen-induced innate immune responses and sterile inflammation (*62*).

An additional important finding of our studies is that the nuclear receptors RORC and PPARγ are up-regulated in myeloid cells by PD-1 ablation. RORs were initially considered retinoic acid receptors but were subsequently identified as sterol ligands. RORC not only is induced by sterols and isoprenoid intermediates (*49*) but also serves as the high-affinity receptor of the cholesterol precursor desmosterol (*63*, *64*), a metabolic intermediate of cholesterol synthesis via the mevalonate pathway that regulates inflammatory responses of myeloid cells (*52*, *60*). Desmosterol and as sterol sulfates function as endogenous RORC agonists and induce expression of RORC target genes (*63*, *64*). Our studies showed that, in addition to cholesterol, the mevalonate metabolism product GGPP that has an active role in the up-regulation of RORC expression (*49*) was elevated in PD-1–deficient myeloid cells, providing a mechanistic basis for our finding of the elevated RORC expression. Retinoid receptors and PPARγ together regulate monocyte/macrophage terminal differentiation (*26*). Although initially thought to be involved in proinflammatory macrophage differentiation, it was subsequently understood that PPARγ predominantly promotes macrophage-mediated resolution of inflammation by inducing expression of the nuclear receptor liver X receptor and the scavenger receptor CD36, thereby regulating tissue remodeling (*65*). PPARγ also regulates macrophage-mediated tissue remodeling by efferocytosis and production of proresolving cytokines (*66*), which can suppress cancer growth (*67*). The combined actions of RORC and PPARγ induced by myeloid-specific PD-1 ablation

might be involved in the antitumor function by promoting both proinflammatory and tissue remodeling properties of myeloid cells. Future studies will dissect the specific role of each of these nuclear receptors on the antitumor immunity induced by myeloid cell–specific ablation of PD-1.

In conclusion, our results provide multiple levels of evidence that myeloid-specific PD-1 targeting mediates myeloid cell–intrinsic effects, which have a decisive role on systemic antitumor responses. This might be a key mechanism by which PD-1 blockade induces antitumor function. Recapitulating this immunometabolic program of myeloid cells will improve the outcome of cancer immunotherapy.

MATERIALS AND METHODS

Animals

All procedures were in accordance with the National Institutes of Health Guidelines for the Care and Use of Animals and approved by the Institutional Animal Care and Use Committee at Beth Israel Deaconess Medical Center (Boston, MA). C57BL/6 WT mice were purchased from Charles River Laboratories (Franklin, MA). PD-1$^{-/-}$ mice were provided by T. Honjo (Kyoto University, Japan). PD-1$^{-/-}$ mice (B6.Cg-*Pdcd1*$^{tm1.1Shr}$/J) were also purchased from the Jackson laboratory (Bar Harbor, ME). All the studies requiring the use of PD-1$^{-/-}$ mice were performed with both PD-1–deficient strains and resulted in similar outcomes. *Pdcd1*$^{flox/flox}$ (PD-1$^{f/f}$) mice on a C57BL/6 background were generated by Ozgene (Australia) using goGermline technology. Briefly, a targeting vector was prepared containing LoxP sites in introns 1 and 3, closely flanking exons 2 and 3, respectively, of the Pdcd1 (fig. S12A). The genomic 5′ and 3′ arms of homology and the floxed genomic region were generated by PCR amplification of C57BL/6 genomic DNA. An Frt-PGK-Neo^{R}-Frt selection cassette was placed immediately 5′ of the LoxP site in intron 3. Homologous recombination of the targeting vector was carried out by electroporation of embryonic stem (ES) cells, and clones were selected for neomycin resistance. Correctly targeted ES clones were identified by Southern blot restriction fragment length polymorphism (RFLP) analysis and microinjected into goGermline blastocysts to generate germline chimeras. After germline transmission, the FRT-PGK-Neo^{R}-FRT cassette was deleted by mating to a transgenic line containing FLP recombinase. The *Flp* gene was removed by segregation in subsequent crosses. PD-1$^{f/f}$ mice were mated with LysMcre mice [B6.129P2^{-} *Lyz2*$^{tm1(cre)Ifo}$/J] or CD4cre mice [B6.Cg-Tg(Cd4-cre)1Cwi/BfluJ], obtained from the Jackson laboratory. Selective ablation of PD-1 protein expression in T cells versus myeloid cells in each strain was confirmed by flow cytometry (fig. S12, B and C). Rag2-deficient mice [B6(Cg)-*Rag2*$^{tm1.1Cgn}$/J], OTI TCR transgenic mice [C57BL/6^{-} Tg(TcraTcrb)1100Mjb/J], and OTII TCR transgenic mice [B6.Cg-Tg(TcraTcrb)425Cbn/J] were purchased from the Jackson laboratory (Bar Harbor, ME).

Tumor cell lines and tumor experiments

MC17-51 and B16-F10 cell lines were purchased from the American Type Culture Collection. The B16-F10 cell line was subcloned, and subclones with intermediate growth rate were selected for use. The MC38 cell line was purchased from Kerafast. For tumor implantation, 10^5 murine fibrosarcoma (MC17-51) were injected intramuscularly in the left hindlimb, whereas 2.5×10^5 murine colon carcinoma (MC38) or 5×10^5 murine melanoma (B16-F10) cells were injected subcutaneously in the left flank. Tumor growth was monitored daily with a caliper fitted with a vernier scale, starting from day 9. Tumor volume was calculated on the basis of three perpendicular measurements. At days 15 to 16 for B16-F10 tumors, at days 12 to 14 for MC17-51 tumors, and at days 15 to 21 for MC38 after tumor inoculation, mice were euthanized, and tumor, spleen, small intestine, and bone marrow were harvested. Eight- to 12-week-old male mice were used for MC17-51 inoculations, and 8- to 12-week-old male or female mice were used for MC38 and B16-F10 inoculations. For studies at various time points after tumor implantation, a large cohort of mice of each strain was used for simultaneous tumor inoculation, and at the indicated times, equal numbers of mice were euthanized and assessment of the indicated end points was performed. For treatment with anti–PD-1–blocking antibody, 250 μg of either anti–PD-1 (clone RMP1-14, Bio X Cell) or immunoglobulin G2a control (clone 2A3, Bio X Cell) diluted in sterile phosphate-buffered saline were administered intraperitoneally in a volume of 100 μl per dose on days 9, 12, and 15 after tumor inoculation.

Statistics

Statistical significance for comparison between two groups was determined by two-tailed Student's *t* test or Mann-Whitney *U* test. Statistical significance for comparison among three or more groups was determined by analysis of variance (ANOVA). $*P < 0.05$, $**P < 0.01$, $***P < 0.005$, and $****P < 0.001$.

SUPPLEMENTARY MATERIALS

immunology.sciencemag.org/cgi/content/full/5/43/eaay1863/DC1

Materials and Methods

Fig. S1. Gating strategy of hematopoietic and myeloid precursors in the bone marrow.

Fig. S2. Gating strategy of myeloid subsets in the spleen and tumor site.

Fig. S3. Cancer-induced emergency myelopoiesis in three different mouse tumor models.

Fig. S4. PD-1 expression is induced on myeloid progenitors by emergency cytokines.

Fig. S5. Gating strategy for identification of MDSC in human blood samples.

Fig. S6. PD-1 expression in human MDSC.

Fig. S7. PD-1 ablation alters tumor-driven emergency myelopoiesis.

Fig. S8. PD-1 ablation induces expression of RORC and IRF8 in myeloid cells expanding in response to tumor-driven emergency myelopoiesis.

Fig. S9. PD-1 ablation induces expression of RORC and IRF8 in myeloid cells expanding in mice-bearing MC38 or MC17-51 tumors.

Fig. S10. PD-1 ablation increases the output of RORC^{hi} effector-like myeloid cells at early stages of tumor growth.

Fig. S11. Therapeutic targeting of PD-1 increases effector features of myeloid cells and decreases tumor growth.

Fig. S12. Myeloid-specific and T cell–specific PD-1 deletion.

Fig. S13. Myeloid-specific PD-1 ablation promotes expansion of IRF8^{hi} and RORC^{hi} monocytes and IFN-γ–producing monocytes and macrophages in the tumor site.

Fig. S14. Tumor-induced emergency myelopoiesis and myeloid effector differentiation in Rag2-deficient mice treated with PD-1 antibody.

Fig. S15. PD-1 ablation reduces the threshold of growth factor–mediated signaling in GMP.

Fig. S16. Myeloid-specific PD-1 ablation induces a distinct metabolic profile characterized by elevated cholesterol.

Fig. S17. Metabolic pathways linking glycolysis to PPP, fatty acid, and cholesterol synthesis.

Fig. S18. Schematic presentation of the mevalonate pathway.

Fig. S19. Increase of glucose uptake and neutral lipid content in PD-1–deficient myeloid progenitors early after tumor implantation.

Fig. S20. Myeloid-specific PD-1 deletion alters the immunological profile of CD8^{+} T_{EM} cells.

Fig. S21. PD-1 ablation enhances antigen presentation ex vivo by tumor-matured DC.

Table S1. List of significantly different metabolites.

Table S2. List of antibodies used for surface staining.

Table S3. List of antibodies used for intracellular staining.

Table S4. List of antibodies used for phenotype of human MDSC.

Table S5. Raw data in Excel spreadsheet.

References (*68*–*71*)

View/request a protocol for this paper from *Bio-protocol*.

REFERENCES AND NOTES

1. T. Okazaki, S. Chikuma, Y. Iwai, S. Fagarasan, T. Honjo, A rheostat for immune responses: The unique properties of PD-1 and their advantages for clinical application. *Nat. Immunol.* **14**, 1212–1218 (2013).
2. V. A. Boussiotis, Molecular and biochemical aspects of the PD-1 checkpoint pathway. *N. Engl. J. Med.* **375**, 1767–1778 (2016).
3. N. A. Rizvi, M. D. Hellmann, A. Snyder, P. Kvistborg, V. Makarov, J. J. Havel, W. Lee, J. Yuan, P. Wong, T. S. Ho, M. L. Miller, N. Rekhtman, A. L. Moreira, F. Ibrahim, C. Bruggeman, B. Gasmi, R. Zappasodi, Y. Maeda, C. Sander, E. B. Garon, T. Merghoub, J. D. Wolchok, T. N. Schumacher, T. A. Chan, Cancer immunology. Mutational landscape determines sensitivity to PD-1 blockade in non-small cell lung cancer. *Science* **348**, 124–128 (2015).
4. W. Chen, J. Wang, L. Jia, J. Liu, Y. Tian, Attenuation of the programmed cell death-1 pathway increases the M1 polarization of macrophages induced by zymosan. *Cell Death Dis.* **7**, e2115 (2016).
5. X. Huang, F. Venet, Y. L. Wang, A. Lepape, Z. Yuan, Y. Chen, R. Swan, H. Kherouf, G. Monneret, C. S. Chung, A. Ayala, PD-1 expression by macrophages plays a pathologic role in altering microbial clearance and the innate inflammatory response to sepsis. *Proc. Natl. Acad. Sci. U.S.A.* **106**, 6303–6308 (2009).
6. L. Shen, Y. Gao, Y. Liu, B. Zhang, Q. Liu, J. Wu, L. Fan, Q. Ou, W. Zhang, L. Shao, PD-1/PD-L pathway inhibits M.tb-specific $CD4^+$ T-cell functions and phagocytosis of macrophages in active tuberculosis. *Sci. Rep.* **6**, 38362 (2016).
7. M. Qorraj, H. Bruns, M. Böttcher, L. Weigand, D. Saul, A. Mackensen, R. Jitschin, D. Mougiakakos, The PD-1/PD-L1 axis contributes to immune metabolic dysfunctions of monocytes in chronic lymphocytic leukemia. *Leukemia* **31**, 470–478 (2017).
8. S. R. Gordon, R. L. Maute, B. W. Dulken, G. Hutter, B. M. George, M. N. McCracken, R. Gupta, J. M. Tsai, R. Sinha, D. Corey, A. M. Ring, A. J. Connolly, I. L. Weissman, PD-1 expression by tumour-associated macrophages inhibits phagocytosis and tumor immunity. *Nature* **545**, 495–499 (2017).
9. D. I. Gabrilovich, S. Ostrand-Rosenberg, V. Bronte, Coordinated regulation of myeloid cells by tumours. *Nat. Rev. Immunol.* **12**, 253–268 (2012).
10. V. Bronte, S. Brandau, S.-H. Chen, M. P. Colombo, A. B. Frey, T. F. Greten, S. Mandruzzato, P. J. Murray, A. Ochoa, S. Ostrand-Rosenberg, P. C. Rodriguez, A. Sica, V. Umansky, R. H. Vonderheide, D. I. Gabrilovich, Recommendations for myeloid-derived suppressor cell nomenclature and characterization standards. *Nat. Commun.* **7**, 12150 (2016).
11. L. Dolcetti, E. Peranzoni, S. Ugel, I. Marigo, A. F. Gomez, C. Mesa, M. Geilich, G. Winkels, E. Traggiai, A. Casati, F. Grassi, V. Bronte, Hierarchy of immunosuppressive strength among myeloid-derived suppressor cell subsets is determined by GM-CSF. *Eur. J. Immunol.* **40**, 22–35 (2010).
12. J. I. Youn, S. Nagaraj, M. Collazo, D. I. Gabrilovich, Subsets of myeloid-derived suppressor cells in tumor-bearing mice. *J. Immunol.* **181**, 5791–5802 (2008).
13. K. Movahedi, M. Guilliams, J. Van den Bossche, R. Van den Bergh, C. Gysemans, A. Beschin, P. De Baetselier, J. A. Van Ginderachter, Identification of discrete tumor-induced myeloid-derived suppressor cell subpopulations with distinct T cell-suppressive activity. *Blood* **111**, 4233–4244 (2008).
14. V. Kumar, S. Patel, E. Tcyganov, D. I. Gabrilovich, The nature of myeloid-derived suppressor cells in the tumor microenvironment. *Trends Immunol.* **37**, 208–220 (2016).
15. P. H. Feng, K.-Y. Lee, Y.-L. Chang, Y.-F. Chan, L.-W. Kuo, T.-Y. Lin, F.-T. Chung, C.-S. Kuo, C.-T. Yu, S.-M. Lin, C.-H. Wang, C.-L. Chou, C.-D. Huang, H.-P. Kuo, $CD14^+S100A9^+$ monocytic myeloid-derived suppressor cells and their clinical relevance in non-small cell lung cancer. *Am. J. Respir. Crit. Care Med.* **186**, 1025–1036 (2012).
16. C. Iclozan, S. Antonia, A. Chiappori, D. T. Chen, D. Gabrilovich, Therapeutic regulation of myeloid-derived suppressor cells and immune response to cancer vaccine in patients with extensive stage small cell lung cancer. *Cancer Immunol. Immunother.* **62**, 909–918 (2013).
17. C. Meyer, L. Cagnon, C. M. Costa-Nunes, P. Baumgaertner, N. Montandon, L. Leyvraz, O. Michielin, E. Romano, D. E. Speiser, Frequencies of circulating MDSC correlate with clinical outcome of melanoma patients treated with ipilimumab. *Cancer Immunol. Immunother.* **63**, 247–257 (2014).
18. I. Azzaoui, F. Uhel, D. Rossille, C. Pangault, J. Dulong, J. L. Priol, T. Lamy, R. Houot, S. L. Gouill, G. Cartron, P. Godmer, K. Bouabdallah, N. Milpied, G. Damaj, K. Tarte, T. Fest, M. Roussel, T-cell defect in diffuse large B-cell lymphomas involves expansion of myeloid-derived suppressor cells. *Blood* **128**, 1081–1092 (2016).
19. R. Weber, V. Fleming, X. Hu, V. Nagibin, C. Groth, P. Altevogt, J. Utikal, V. Umansky, Myeloid-derived suppressor cells hinder the anti-cancer activity of immune checkpoint inhibitors. *Front. Immunol.* **9**, 1310 (2018).
20. D. Pan, A. Kobayashi, P. Jiang, L. F. de Andrade, R. E. Tay, A. M. Luoma, D. Tsoucas, X. Qiu, K. Lim, P. Rao, H. W. Long, G.-C. Yuan, J. Doench, M. Brown, X. S. Liu, K. W. Wucherpfennig, A major chromatin regulator determines resistance of tumor cells to T cell-mediated killing. *Science* **359**, 770–775 (2018).
21. L. Strauss, S. Sangaletti, F. M. Consonni, G. Szebeni, S. Morlacchi, M. G. Totaro, C. Porta, A. Anselmo, S. Tartari, A. Doni, F. Zitelli, C. Tripodo, M. P. Colombo, A. Sica, RORC1 regulates tumor-promoting "emergency" granulo-monocytopoiesis. *Cancer Cell* **28**, 253–269 (2015).
22. D. Sichien, C. L. Scott, L. Martens, M. Vanderkerken, S. Van Gassen, M. Plantinga, T. Joeris, S. De Prijck, L. Vanhoutte, M. Vanheerswynghels, G. Van Isterdael, W. Toussaint, F. B. Madeira, K. Vergote, W. W. Agace, B. E. Clausen, H. Hammad, M. Dalod, Y. Saeys, B. N. Lambrecht, M. Guilliams, IRF8 transcription factor controls survival and function of terminally differentiated conventional and plasmacytoid dendritic cells, respectively. *Immunity* **45**, 626–640 (2016).
23. A. Yanez, M. Y. Ng, N. Hassanzadeh-Kiabi, H. S. Goodridge, IRF8 acts in lineage-committed rather than oligopotent progenitors to control neutrophil vs monocyte production. *Blood* **125**, 1452–1459 (2015).
24. C. S. Netherby, M. N. Messmer, L. Burkard-Mandel, S. Colligan, A. Miller, E. C. Gomez, J. Wang, M. J. Nemeth, S. I. Abrams, The granulocyte progenitor stage is a key target of IRF8-mediated regulation of myeloid-derived suppressor cell production. *J. Immunol.* **198**, 4129–4139 (2017).
25. J. D. Waight, C. Netherby, M. L. Hensen, A. Miller, Q. Hu, S. Liu, P. N. Bogner, M. R. Farren, K. P. Lee, K. Liu, S. I. Abrams, Myeloid-derived suppressor cell development is regulated by a STAT/IRF-8 axis. *J. Clin. Invest.* **123**, 4464–4478 (2013).
26. A. Szanto, L. Nagy, Retinoids potentiate peroxisome proliferator-activated receptor γ action in differentiation, gene expression, and lipid metabolic processes in developing myeloid cells. *Mol. Pharmacol.* **67**, 1935–1943 (2005).
27. P. L. Raber, P. Thevenot, R. Sierra, D. Wyczechowska, D. Halle, M. E. Ramirez, A. C. Ochoa, M. Fletcher, C. Velasco, A. Wilk, K. Reiss, P. C. Rodriguez, Subpopulations of myeloid-derived suppressor cells impair T cell responses through independent nitric oxide-related pathways. *Int. J. Cancer* **134**, 2853–2864 (2014).
28. S. Mandruzzato, S. Solito, E. Falisi, S. Francescato, V. Chiarion-Sileni, S. Mocellin, A. Zanon, C. R. Rossi, D. Nitti, V. Bronte, P. Zanovello, $IL4R\alpha^+$ myeloid-derived suppressor cell expansion in cancer patients. *J. Immunol.* **182**, 6562–6568 (2009).
29. V. Bronte, P. Serafini, C. De Santo, I. Marigo, V. Tosello, A. Mazzoni, D. M. Segal, C. Staib, M. Lowel, G. Sutter, M. P. Colombo, P. Zanovello, IL-4-induced arginase 1 suppresses alloreactive T cells in tumor-bearing mice. *J. Immunol.* **170**, 270–278 (2003).
30. C. Giallongo, N. Parrinello, D. Tibullo, P. L. Cava, A. Romano, A. Chiarenza, I. Barbagallo, G. A. Palumbo, F. Stagno, P. Vigneri, F. D. Raimondo, Myeloid derived suppressor cells (MDSCs) are increased and exert immunosuppressive activity together with polymorphonuclear leukocytes (PMNs) in chronic myeloid leukemia patients. *PLOS ONE* **9**, e101848 (2014).
31. J. M. Zou, J. Qin, Y. C. Li, Y. Wang, D. Li, Y. Shu, C. Luo, S. S. Wang, G. Chi, F. Guo, G. M. Zhang, Z. H. Feng, IL-35 induces N2 phenotype of neutrophils to promote tumor growth. *Oncotarget* **8**, 33501–33514 (2017).
32. J. Woytschak, N. Keller, C. Krieg, D. Impellizzieri, R. W. Thompson, T. A. Wynn, A. S. Zinkernagel, O. Boyman, Type 2 interleukin-4 receptor signaling in neutrophils antagonizes their expansion and migration during infection and inflammation. *Immunity* **45**, 172–184 (2016).
33. G. Mondanelli, R. Bianchi, M. T. Pallotta, C. Orabona, E. Albini, A. Iacono, M. L. Belladonna, C. Vacca, F. Fallarino, A. Macchiarulo, S. Ugel, V. Bronte, F. Gevi, L. Zolla, A. Verhaar, M. Peppelenbosch, E. M. C. Mazza, S. Bicciato, Y. Laouar, L. Santambrogio, P. Puccetti, C. Volpi, U. Grohmann, A relay pathway between arginine and tryptophan metabolism confers immunosuppressive properties on dendritic cells. *Immunity* **46**, 233–244 (2017).
34. R. V. Parry, J. M. Chemnitz, K. A. Frauwirth, A. R. Lanfranco, I. Braunstein, S. V. Kobayashi, P. S. Linsley, C. B. Thompson, J. L. Riley, CTLA-4 and PD-1 receptors inhibit T-cell activation by distinct mechanisms. *Mol. Cell. Biol.* **25**, 9543–9553 (2005).
35. N. Patsoukis, J. Brown, V. Petkova, F. Liu, L. Li, V. A. Boussiotis, Selective effects of PD-1 on Akt and Ras pathways regulate molecular components of the cell cycle and inhibit T cell proliferation. *Sci. Signal.* **5**, ra46 (2012).
36. M. Ye, H. Iwasaki, C. V. Laiosa, M. Stadtfeld, H. Xie, S. Heck, B. Clausen, K. Akashi, T. Graf, Hematopoietic stem cells expressing the myeloid lysozyme gene retain long-term, multilineage repopulation potential. *Immunity* **19**, 689–699 (2003).
37. G. J. Lieschke, D. Grail, G. Hodgson, D. Metcalf, E. Stanley, C. Cheers, K. J. Fowler, S. Basu, Y. F. Zhan, A. R. Dunn, Mice lacking granulocyte colony-stimulating factor have chronic neutropenia, granulocyte and macrophage progenitor cell deficiency, and impaired neutrophil mobilization. *Blood* **84**, 1737–1746 (1994).
38. F. Liu, H. Y. Wu, R. Wesselschmidt, T. Kornaga, D. C. Link, Impaired production and increased apoptosis of neutrophils in granulocyte colony-stimulating factor receptor-deficient mice. *Immunity* **5**, 491–501 (1996).
39. S. H. Albeituni, C. Ding, M. Liu, X. Hu, F. Luo, G. Kloecker, M. Bousamra II, H.-g. Zhang, J. Yan, Yeast-derived particulate β-glucan treatment subverts the suppression of myeloid-derived suppressor cells (MDSC) by inducing polymorphonuclear MDSC apoptosis and monocytic MDSC differentiation to APC in cancer. *J. Immunol.* **196**, 2167–2180 (2016).
40. D. Li, H. Yang, H. Nan, P. Liu, S. Pang, Q. Zhao, R. Karni, M. P. Kamps, Y. Xu, J. Zhou, T. Wiedmer, P. J. Sims, F. Wang, Identification of key regulatory pathways of myeloid

differentiation using an mESC-based karyotypically normal cell model. *Blood* **120**, 4712–4719 (2012).
41. P. W. F. Karmaus, A. A. Herrada, C. Guy, G. Neale, Y. Dhungana, L. Long, P. Vogel, J. Avila, C. B. Clish, H. Chi, Critical roles of mTORC1 signaling and metabolic reprogramming for M-CSF-mediated myelopoiesis. *J. Exp. Med.* **214**, 2629–2647 (2017).
42. E. M. Coccia, N. D. Russo, E. Stellacci, U. Testa, G. Marziali, A. Battistini, STAT1 activation during monocyte to macrophage maturation: Role of adhesion molecules. *Int. Immunol.* **11**, 1075–1083 (1999).
43. A. Moussaieff, M. Rouleau, D. Kitsberg, M. Cohen, G. Levy, D. Barasch, A. Nemirovski, S. Shen-Orr, I. Laevsky, M. Amit, D. Bomze, B. Elena-Herrmann, T. Scherf, M. Nissim-Rafinia, S. Kempa, J. Itskovitz-Eldor, E. Meshorer, D. Aberdam, Y. Nahmias, Glycolysis-mediated changes in acetyl-CoA and histone acetylation control the early differentiation of embryonic stem cells. *Cell Metab.* **21**, 392–402 (2015).
44. T. TeSlaa, A. C. Chaikovsky, I. Lipchina, S. L. Escobar, K. Hochedlinger, J. Huang, T. G. Graeber, D. Braas, M. A. Teitell, α-Ketoglutarate accelerates the initial differentiation of primed human pluripotent stem cells. *Cell Metab.* **24**, 485–493 (2016).
45. W. M. Yu, X. Liu, J. Shen, O. Jovanovic, E. E. Pohl, S. L. Gerson, T. Finkel, H. E. Broxmeyer, C.-K. Qu, Metabolic regulation by the mitochondrial phosphatase PTPMT1 is required for hematopoietic stem cell differentiation. *Cell Stem Cell* **12**, 62–74 (2013).
46. K. Ito, K. Ito, Hematopoietic stem cell fate through metabolic control. *Exp. Hematol.* **64**, 1–11 (2018).
47. K. Duvel, J. L. Yecies, S. Menon, P. Raman, A. I. Lipovsky, A. L. Souza, E. Triantafellow, Q. Ma, R. Gorski, S. Cleaver, M. G. Vander Heiden, J. P. Mac Keigan, P. M. Finan, C. B. Clish, L. O. Murphy, B. D. Manning, Activation of a metabolic gene regulatory network downstream of mTOR complex 1. *Mol. Cell* **39**, 171–183 (2010).
48. T. Porstmann, B. Griffiths, Y.-L. Chung, O. Delpuech, J. R. Griffiths, J. Downward, A. Schulze, PKB/Akt induces transcription of enzymes involved in cholesterol and fatty acid biosynthesis via activation of SREBP. *Oncogene* **24**, 6465–6481 (2005).
49. S. Kagami, T. Owada, H. Kanari, Y. Saito, A. Suto, K. Ikeda, K. Hirose, N. Watanabe, I. Iwamoto, H. Nakajima, Protein geranylgeranylation regulates the balance between Th17 cells and Foxp3$^+$ regulatory T cells. *Int. Immunol.* **21**, 679–689 (2009).
50. A. J. Murphy, M. Akhtari, S. Tolani, T. Pagler, N. Bijl, C.-L. Kuo, M. Wang, M. Sanson, S. Abramowicz, C. Welch, A. E. Bochem, J. A. Kuivenhoven, L. Yvan-Charvet, A. R. Tall, ApoE regulates hematopoietic stem cell proliferation, monocytosis, and monocyte accumulation in atherosclerotic lesions in mice. *J. Clin. Invest.* **121**, 4138–4149 (2011).
51. M. Westerterp, E. L. Gautier, A. Ganda, M. M. Molusky, W. Wang, P. Fotakis, N. Wang, G. J. Randolph, V. D. D'Agati, L. Yvan-Charvet, A. R. Tall, Cholesterol accumulation in dendritic cells links the inflammasome to acquired immunity. *Cell Metab.* **25**, 1294–1304.e6 (2017).
52. A. R. Tall, L. Yvan-Charvet, Cholesterol, inflammation and innate immunity. *Nat. Rev.* **15**, 104–116 (2015).
53. P. Tontonoz, L. Nagy, J. G. Alvarez, V. A. Thomazy, R. M. Evans, PPARγ promotes monocyte/macrophage differentiation and uptake of oxidized LDL. *Cell* **93**, 241–252 (1998).
54. N. E. Scharping, A. V. Menk, R. S. Moreci, R. D. Whetstone, R. E. Dadey, S. C. Watkins, R. L. Ferris, G. M. Delgoffe, The tumor microenvironment represses T cell mitochondrial biogenesis to drive intratumoral T cell metabolic insufficiency and dysfunction. *Immunity* **45**, 374–388 (2016).
55. J. S. Bowers, M. H. Nelson, K. Majchrzak, S. R. Bailey, B. Rohrer, A. D. M. Kaiser, C. Atkinson, L. Gattinoni, C. M. Paulos, Th17 cells are refractory to senescence and retain robust antitumor activity after long-term ex vivo expansion. *JCI Insight* **2**, e90772 (2017).
56. S. Chatterjee, A. Daenthanasanmak, P. Chakraborty, M. W. Wyatt, P. Dhar, S. P. Selvam, J. Fu, J. Zhang, H. Nguyen, I. Kang, K. Toth, M. Al-Homrani, M. Husain, G. Beeson, L. Ball, K. Helke, S. Husain, E. Garrett-Mayer, G. Hardiman, M. Mehrotra, M. I. Nishimura, C. C. Beeson, M. G. Bupp, J. Wu, B. Ogretmen, C. M. Paulos, J. Rathmell, X. Z. Yu, S. Mehrotra, CD38-NAD$^+$axis regulates immunotherapeutic anti-tumor T cell response. *Cell Metab.* **27**, 85–100e8 (2018).
57. A. W.-M. Lee, D. J. States, Colony-stimulating factor-1 requires PI3-kinase-mediated metabolism for proliferation and survival in myeloid cells. *Cell Death Differ.* **13**, 1900–1914 (2006).
58. M. Buitenhuis, L. P. Verhagen, H. W. M. van Deutekom, A. Castor, S. Verploegen, L. Koenderman, S.-E. W. Jacobsen, P. J. Coffer, Protein kinase B (c-akt) regulates hematopoietic lineage choice decisions during myelopoiesis. *Blood* **111**, 112–121 (2008).
59. J. T. Rodgers, K. Y. King, J. O. Brett, M. J. Cromie, G. W. Charville, K. K. Maguire, C. Brunson, N. Mastey, L. Liu, C.-R. Tsai, M. A. Goodell, T. A. Rando, mTORC1 controls the adaptive transition of quiescent stem cells from G0 to G_{Alert}. *Nature* **510**, 393–396 (2014).
60. N. J. Spann, L. X. Garmire, J. G. McDonald, D. S. Myers, S. B. Milne, N. Shibata, D. Reichart, J. N. Fox, I. Shaked, D. Heudobler, C. R. H. Raetz, E. W. Wang, S. L. Kelly, M. C. Sullards, R. C. Murphy, A. H. Merrill Jr., H. A. Brown, E. A. Dennis, A. C. Li, K. Ley, S. Tsimikas, E. Fahy, S. Subramaniam, O. Quehenberger, D. W. Russell, C. K. Glass, Regulated accumulation of desmosterol integrates macrophage lipid metabolism and inflammatory responses. *Cell* **151**, 138–152 (2012).
61. H. A. Anderson, P. A. Roche, MHC class II association with lipid rafts on the antigen presenting cell surface. *Biochim. Biophys. Acta* **1853**, 775–780 (2015).
62. K. Y. King, M. A. Goodell, Inflammatory modulation of HSCs: Viewing the HSC as a foundation for the immune response. *Nat. Rev. Immunol.* **11**, 685–692 (2011).
63. X. Hu, Y. Wang, L.-Y. Hao, X. Liu, C. A. Lesch, B. M. Sanchez, J. M. Wendling, R. W. Morgan, T. D. Aicher, L. L. Carter, P. L. Toogood, G. D. Glick, Sterol metabolism controls T_H17 differentiation by generating endogenous RORγ agonists. *Nat. Chem. Biol.* **11**, 141–147 (2015).
64. F. R. Santori, P. Huang, S. A. van de Pavert, E. F. Douglass Jr., D. J. Leaver, B. A. Haubrich, R. Keber, G. Lorbek, T. Konijn, B. N. Rosales, D. Rozman, S. Horvat, A. Rahier, R. E. Mebius, F. Rastinejad, W. D. Nes, D. R. Littman, Identification of natural RORγ ligands that regulate the development of lymphoid cells. *Cell Metab.* **21**, 286–297 (2015).
65. A. Chawla, W. A. Boisvert, C.-H. Lee, B. A. Laffitte, Y. Barak, S. B. Joseph, D. Liao, L. Nagy, P. A. Edwards, L. K. Curtiss, R. M. Evans, P. Tontonoz, A PPAR γ-LXR-ABCA1 pathway in macrophages is involved in cholesterol efflux and atherogenesis. *Mol. Cell* **7**, 161–171 (2001).
66. Y. S. Yoon, S.-Y. Kim, M.-J. Kim, J.-H. Lim, M.-S. Cho, J. L. Kang, PPARγ activation following apoptotic cell instillation promotes resolution of lung inflammation and fibrosis via regulation of efferocytosis and proresolving cytokines. *Mucosal Immunol.* **8**, 1031–1046 (2015).
67. M. L. Sulciner, C. N. Serhan, M. M. Gilligan, D. K. Mudge, J. Chang, A. Gartung, K. A. Lehner, D. R. Bielenberg, B. Schmidt, J. Dalli, E. R. Greene, Y. Gus-Brautbar, J. Piwowarski, T. Mammoto, D. Zurakowski, M. Perretti, V. P. Sukhatme, A. Kaipainen, M. W. Kieran, S. Huang, D. Panigrahy, Resolvins suppress tumor growth and enhance cancer therapy. *J. Exp. Med.* **215**, 115–140 (2018).
68. I. Zanoni, R. Ostuni, G. Capuano, M. Collini, M. Caccia, A. E. Ronchi, M. Rocchetti, F. Mingozzi, M. Foti, G. Chirico, B. Costa, A. Zaza, P. Ricciardi-Castagnoli, F. Granucci, CD14 regulates the dendritic cell life cycle after LPS exposure through NFAT activation. *Nature* **460**, 264–268 (2009).
69. B. Weigmann, I. Tubbe, D. Seidel, A. Nicolaev, C. Becker, M. F. Neurath, Isolation and subsequent analysis of murine lamina propria mononuclear cells from colonic tissue. *Nat. Protoc.* **2**, 2307–2311 (2007).
70. C. A. Dumitru, K. Moses, S. Trellakis, S. Lang, S. Brandau, Neutrophils and granulocytic myeloid-derived suppressor cells: Immunophenotyping, cell biology and clinical relevance in human oncology. *Cancer Immunol. Immunother.* **61**, 1155–1167 (2012).
71. M. Yuan, S. B. Breitkopf, X. Yang, J. M. Asara, A positive/negative ion-switching, targeted mass spectrometry-based metabolomics platform for bodily fluids, cells, and fresh and fixed tissue. *Nat. Protoc.* **7**, 872–881 (2012).

Acknowledgments
Funding: This work was supported by NIH grants CA183605, CA183605S1, and AI098129-01 and by the DoD grant PC140571. **Author contribution:** L.S. participated in the conceptualization of the project and experimental design, performed experiments and the analysis and validation of the data, prepared figures, and participated in the preparation of the manuscript. M.A.A.M. performed experiments and the analysis and validation of the data, prepared figures, and participated in the preparation of the manuscript. J.D.W., N.M.T.-O., A.C., R.P., Q.W., and M.Y. participated in various steps of the experimental studies. J.A. participated in the experimental design of metabolite studies and the formal analysis and the validation of the data and participated in the preparation of the manuscript. N.P. participated in the conceptualization of the project, designed and performed the bioenergetics studies, and participated in experiments, the analysis and validation of the data, and the preparation of the manuscript. V.A.B. had the overall responsibility of project conceptualization, experimental design, investigation, data analysis and validation, and preparation of the manuscript and figures. **Competing interests:** V.A.B. has patents on the PD-1 pathway licensed by Bristol-Myers Squibb, Roche, Merck, EMD-Serono, Boehringer Ingelheim, AstraZeneca, Novartis, and Dako. The authors declare no other competing interests. **Data and materials availability:** All data needed to evaluate the conclusions in the paper are present in the paper or the Supplementary Materials.

Submitted 29 May 2019
Accepted 13 November 2019
Published 3 January 2020
10.1126/sciimmunol.aay1863

Citation: L. Strauss, M. A. A. Mahmoud, J. D. Weaver, N. M. Tijaro-Ovalle, A. Christofides, Q. Wang, R. Pal, M. Yuan, J. Asara, N. Patsoukis, V. A. Boussiotis, Targeted deletion of PD-1 in myeloid cells induces antitumor immunity. *Sci. Immunol.* **5**, eaay1863 (2020).

Science Immunology

Targeted deletion of PD-1 in myeloid cells induces antitumor immunity

Laura Strauss, Mohamed A. A. Mahmoud, Jessica D. Weaver, Natalia M. Tijaro-Ovalle, Anthos Christofides, Qi Wang, Rinku Pal, Min Yuan, John Asara, Nikolaos Patsoukis and Vassiliki A. Boussiotis

Sci. Immunol. **5**, eaay1863.
DOI: 10.1126/sciimmunol.aay1863

A twist in the PD-1 tale

Immunotherapies targeting programmed cell death protein 1 (PD-1) that can reverse T cell exhaustion have revolutionized the treatment of cancer. Here, by generating *Pdcd1* floxed mice and conditionally deleting PD-1 in T cells or in myeloid cells, Strauss *et al*. have uncovered a previously unappreciated role for PD-1 expressed on myeloid cells in dampening antitumor immunity. They found that selective ablation of PD-1 in myeloid cells was just as effective at limiting tumor growth as global deletion of PD-1 and have documented the importance of PD-1 in regulating the development and functions of myeloid cells. Although the study does not question the role of PD-1 in T cell exhaustion, the results call for a rethink of how PD-1–centric therapies work.

Science Immunology (ISSN 2470-9468) is published by the American Association for the Advancement of Science, 1200 New York Avenue NW, Washington, DC 20005. The title *Science Immunology* is a registered trademark of AAAS.